3-D Double-Directional Radio Channel Characterisation for Urban Macrocellular Applications

Kimmo Kalliola, Heikki Laitinen, Pertti Vainikainen, *Member, IEEE*, Martin Toeltsch, *Member, IEEE*, Juha Laurila, *Member, IEEE*, Ernst Bonek, *Senior Member, IEEE*

***Abstract*—We measured the spatial properties of the 3-D double-directional radio channel in urban macrocell environments separately at both ends of the link. In this paper we study propagation conditions pertaining to reception and transmission at the mobile terminal, measured using a wideband channel sounder and a dual-polarised spherical antenna array. We were able to refine the results of the measurements conducted at the base station, and extend the study to full double-directional 3-D channels. Individual propagation paths could be identified precisely, in some cases even considerable scattering from lampposts was observed. Our results show that over-rooftop-dominated propagation often occurs via building roofs with LOS to the base station antenna, acting as strong secondary signal sources. Based on measurements along continuous routes we demonstrate that the dominant propagation mechanisms can vary considerably when the mobile moves in the environment. We also present typical directional properties of the 3-D radio channel at the mobile terminal in urban macrocell environments characterised by street canyons, showing how the angular distribution of energy is correlated with the excess delay.**

***Index Terms*—Mobile radio channel, Double-directional, Radio channel measurements, Direction of arrival estimation, Radio propagation**

Manuscript received April 4, 2002. This work was supported in part by the National Technology Agency of Finland (TEKES), the Graduate School in Electronics, Telecommunications and Automation (GETA), and Fonds zur Förderung der wissenschaftlichen Forschung, Vienna, Austria. Financial support was also received from HPY Foundation, the Finnish Society of Electronics Engineers, and the Finnish Foundation of Technology.

K. Kalliola was with the Institute of Digital Communications (IDC)/Radio Laboratory, Helsinki University of Technology, Espoo, Finland. He is now with Nokia Research Center, Radio Communications Laboratory, Helsinki, Finland (e-mail: kimmo.kalliola@nokia.com).

H. Laitinen is with VTT Information Technology, Telecommunications, Espoo, Finland (e-mail: heikki.laitinen@vtt.fi).

P. Vainikainen is with the Institute of Digital Communications (IDC)/Radio Laboratory, Helsinki University of Technology, Espoo, Finland (e-mail: pertti.vainikainen@hut.fi).

M. Toeltsch was with the Institut für Nachrichtentechnik und Hochfrequenztechnik (INTHF), Tecnische Universität Wien, Vienna, Austria. He is now with SYMENA Software und Consulting GmbH, Vienna, Austria (e-mail: martin.toeltsch@symena.com).

J. Laurila is with Nokia Research Center, Radio Communications Laboratory, Helsinki, Finland.(e-mail: juha.k.laurila@nokia.com).

E. Bonek is with with the Institut für Nachrichtentechnik und Hochfrequenztechnik (INTHF), Tecnische Universität Wien, Vienna, Austria, and also with the Forschungszentrum Telekommunikation Wien (FTW), Vienna, Austria (e-mail: ernst.bonek@tuwien.ac.at).

I. Introduction

Future mobile communication systems will exploit the spatial properties of the radio channel by introducing antenna arrays at the base and/or mobile stations of cellular networks [1,2,3]. For the optimal design of array-processing algorithms, a thorough knowledge of the spatial radio propagation channel is crucial. An introduction to different channel modelling approaches can be found in [4]. In recent years, the European COST (Co-operation in Science and Technology) Action 259, named "Wireless Flexible Personalized Communications" [5], has developed a set of channel models that include the spatial properties of the radio channel. The models are in effect double-directional [6], in the sense that they include consideration of the Directions-of-Arrival (DoAs) of the multipath components at both the base and mobile stations.

Single- and double-directional radio channel measurements are needed for validation of such channel models and for extraction of suitable parameter values for different types of propagation environments and cell sizes. At the mobile terminal the radio environment is three-dimensional [7,8,9]. With the development of better instrumentation it is now possible to measure angles of arrival in both azimuth and elevation planes at the mobile terminal in addition to multipath delays, enabling the development of more accurate models of the type needed for modern spatial array processing. In addition, 3-D double-directional radio channel measurements allow reliable tracking of propagation paths with up to three multiple reflections/diffractions [6,8]. The last interaction points between physical objects and electromagnetic waves before the waves reach the base and mobile stations can be identified precisely, which enables the investigations of different physical propagation mechanisms in urban environments [10,11,12]. This information is highly valuable when evaluating and further developing deterministic propagation models, such as those based on ray tracing [11]. Few double-directional channel measurements have been reported so far, one example can be found in [6].

We carried out two separate measurement campaigns in downtown Helsinki. In the first campaign, reported in [10], we measured the 3-D directional radio channel at the *base*

station (BS) by applying a measurement concept, which was a combination of RF-multiplexing and synthetic aperture techniques in order to form a virtual planar array. The results of the second measurement campaign are presented in this paper. We measured the 3-D radio channel at the *mobile station* (MS) by using a measurement method based on a spherical dual-polarised antenna array. A subset of the BS–MS position pairs considered in [10] were also considered in this work in order to be able to resolve the propagation paths in the double-directional radio channel between the mobile and base stations in urban macrocell environment. Whereas only static measurements were performed in [10], we also performed measurements along continuous mobile routes, to investigate the variation of the radio channel at the mobile station. The first results of these mobile measurements were presented in [13].

In this contribution, we will verify the observations made in [10] and show that in some cases the true propagation paths only became apparent after analysis of the measurements from both ends of the link. We will demonstrate how the dominant propagation mechanisms vary when the mobile terminal moves in the environment, and show how the building height is in connection with the propagation of waves which arrive from over rooftops, then impinge on the top edges of building walls and are diffracted into street canyons. In addition, we will further investigate the 3-D directional radio channel at the mobile terminal, by showing the distribution of power in elevation, and the correlation of the angular power profile and excess delay in an urban environment characterised by street canyons.

Section II describes the measurement concept and post-processing of the data. Section III gives an overview of the measurement environment. In Section IV we present sample results of the 3-D radio channel at the mobile terminal, and compare the results with the measurements at the BS, presented in [10], to obtain double-directional channels. In Section V we investigate the consistency of the propagation paths, and Section VI presents the correlation between the angular power profiles and propagation delay. Section VII summarises and concludes the work.

II. Measurement Concept

A. General

We obtained the angle resolved impulse response of the wideband radio channel at the mobile terminal by using the measurement method presented in [14]. The method is based on the analysis of data measured using a spherical array of 32 dual-polarised antenna elements and a complex wideband radio channel sounder. At the BS, a wideband signal was transmitted using a single fixed vertically polarised (VP) antenna. At the MS the signal was received separately from the θ- and ϕ-polarised feeds of each of the 32 elements of the spherical array, using a fast 64-channel RF switch. The array elements are microstrip patches and their 6-dB beamwidth, measured in-situ in the array, is approximately 90° in the E-plane and 100° in the H-plane. The gain of the element is 7.8 dBi. The cross-polarisation discrimination (XPD) of the element is higher than 18 dB over the 6-dB beamwidth, and the measured XPD of the spherical array is 17 dB and the XPD has a ±4 dB peak-to-peak ripple as a function of the incidence angle [14].

To evaluate the influence of mutual coupling between the elements of the array on its radiation characteristics, the radiation pattern of a single antenna element was measured both in-situ in the array and apart. No significant changes in the radiation were observed: the shape of the main lobe was preserved, as well as the front-to-back ratio, which was roughly 15 dB in both cases. The mean sidelobe level in the region from ±90° to ±150° off the main beam direction increased by some 5 dB when the element was placed in the array. The minimum XPD inside the 6-dB beamwidth decreased from 25 dB to 20 dB in the E-plane and from 19 to 18 dB in the H-plane. There was no significant change in the feedpoint impedance. Based on the above, we conclude that the mutual coupling effects do not significantly degrade the array performance.

Compared to the synthetic aperture technique also applied for 3-D radio channel measurements at the mobile station [7,8,15], the measurement is very fast, and enables acquisition of large data pools from continuous measurement routes. We present results of static measurements for the basis of investigation of individual propagation paths. We also demonstrate how the power carried by a single propagation path changes when the mobile terminal moves by using data measured along a continuous route. Results averaged over a large number of measurement routes to obtain statistical significance are also presented.

During the measurements the array was placed on a trolley, so that its centre was at height of 1.7 m above ground level. In static measurement locations 100 snapshots of the received signal were sampled in a time period of 2.5 s, and the samples were averaged in post processing. In the mobile measurement routes, approximately five snapshots[1] of the received signal were sampled and stored per each wavelength the trolley moved. During the measurement campaign, the transmitting antenna was placed in two different fixed locations corresponding to typical BS antenna installations in urban macrocells. A modified commercial GSM1800 sector antenna with 10 dBi gain and 3 dB beamwidth of 80° in azimuth and 28° in elevation was used, with no tilting. The transmitted power was +40 dBm.

B. Channel Sounder

We used the wideband radio channel sounder described in [16]. In the transmitter, a cyclic pseudo-noise sequence (m-sequence) modulated the carrier at 2.154 GHz. The chip frequency of the m-sequence was 30 MHz in all

[1] each including data from one PN sequence period on each of the 64 channels

measurements leading to a delay resolution of 33 ns. An m-sequence length of 255 chips was chosen, leading to a maximum delay of 8.5 μs. This delay window was found adequate in the measurement environment. In the receiver, the demodulated signal was divided into I- and Q- branches and sampled with two 120 MHz A/D-converters. Sequential sampling over time intervals corresponding to multiple sequence lengths enabled continuous measurement at high sampling rate inside the sampling window. The signal samples from each spherical array element were then stored for off-line processing to compute the temporal and angular information.

Since there is no common reference clock for the sounder transmitter and receiver, the absolute propagation delay was obtained by making a line-of-sight (LOS) measurement with a known distance between the antennas and using that as reference. The local oscillators of the transmitter and receiver were locked to stable Rubidium frequency standards to minimise the drifting of the delay reference during the measurements.

C. Processing of Data

The delays, DoAs, amplitudes, and phases of both θ- and ϕ-polarised components of the incoming waves at each measurement snapshot were estimated through sequential delay-domain and angular-domain processing. Delay-domain processing involves the correlation of the received signal from each antenna element with an ideal copy of the transmitted m-sequence, which yields the complex impulse response estimate of the radio channel. The impulse response estimated from data received by the θ-polarised feed of the n^{th} element is written as

$$h_n^\theta(\tau) = \sum_{i=1}^{4M} h_n^\theta(\tau_i)\delta(\tau_i) \tag{1}$$

where M is the length of the transmitted m-sequence and τ_i is the i^{th} delay tap (four samples per chip period were taken). Similarly, the impulse responses estimated from the ϕ-polarised channels are denoted by superscript ϕ. From the impulse response estimates the power delay profile (PDP) corresponding to one snapshot was computed as:

$$PDP(\tau_i) = \tfrac{1}{32}\sum_{n=1}^{32} |\, h_n^\theta(\tau_i)\,|^2 + |\, h_n^\phi(\tau_i)\,|^2 \tag{2}$$

The reason for summing the squared magnitudes of the impulse response estimates of the θ- and ϕ-polarised feeds of the array elements pointing to different directions was to estimate the PDP corresponding to an isotropic antenna, and thus collect the energy arriving from all directions in space. From the PDP, the delay taps were detected as local maxima exceeding a threshold level. Since there is a considerable variation in the number of received multipath components, it is not appropriate to use a fixed threshold value below the PDP maximum [16]. Instead, a threshold value was calculated by finding the maximum value in a silent interval in the PDP, and adding a 2 dB margin. However, the threshold was never below −27 dB relative to the maximum of the PDP.

The instantaneous θ-polarised spatial response of each delay tap (τ_p) was computed as

$$S^\theta(\theta,\phi,\tau_p) = \sum_{n=1}^{32} w_n(\theta,\phi)\left[u_n^\theta(\theta,\phi)h_n^\theta(\tau_p) + v_n^\theta(\theta,\phi)h_n^\phi(\tau_p)\right] \tag{3}$$

where θ and ϕ define the steering direction in elevation and azimuth, respectively. $w_n(\theta,\phi)$ is a weight factor composed of element phasing and an exponential tapering function, and coefficients $u_n^\theta(\theta,\phi)$ and $v_n^\theta(\theta,\phi)$ are applied in order to orient the elements to receive θ polarisation from the steering direction (see [14] for more details). A grid with beam spacing of 2°in both azimuth and elevation domains was used in the processing. The ϕ-polarised spatial response of each local maximum was computed similarly. The azimuth-elevation-delay-power profile for each snapshot was then computed as

$$P(\theta,\phi,\tau_p) = |\, S^\theta(\theta,\phi,\tau_p)\,|^2 + |\, S^\phi(\theta,\phi,\tau_p)\,|^2 \tag{4}$$

The θ- and ϕ-polarised spatial responses were summed in order to collect received power for directional estimates independently of the polarisation state of the received signal. Corresponding to each delay tap, there may exist one multipath component or several components that are separated by their DoAs. Four multipath components per delay tap were estimated, but only such components were accepted whose amplitude exceeded a threshold value of 6 dB below the highest component, in order to filter out spurious signals due to sidelobes of the array. The measured sidelobe level of the array is approximately −10 dB in the case of two multipath components with equal delays and an angular separation of approximately 40° [14], but the level increases with an increasing number of multipath components.

In addition to the DoAs of the incoming waves, we also obtained the amplitudes and phases of the θ- and ϕ-polarised components of these waves as the values of $S^\theta(\theta,\varphi,\tau_p)$ and $S^\varphi(\theta,\varphi,\tau_p)$ in the directions of local maxima. As a final result, we obtained for each measurement snapshot the angle resolved impulse response estimate, defined as:

$$\begin{bmatrix} h^\theta(\theta,\phi,\tau) \\ h^\phi(\theta,\phi,\tau) \end{bmatrix} = \sum_{l=1}^{L} \begin{bmatrix} \alpha_l^\theta \\ \alpha_l^\phi \end{bmatrix} \delta(\theta-\theta_l)\delta(\phi-\phi_l)\delta(\tau-\tau_l) \tag{5}$$

where h^θ and h^ϕ denote the θ- and ϕ-polarised components of the impulse response, respectively. α_l^θ and

α_l^{ϕ} are the complex amplitudes of l^{th} multipath component, θ_l and ϕ_l are the corresponding elevation and azimuth angles, and τ_1 is the delay.

D. Measurement Accuracy

The directional properties of the measurement system were analysed in [14] by measuring a known radio channel in a radio anechoic chamber. The main drawback of the spherical array is its poor angular resolution and limited angular dynamic range, which is determined by the sidelobes of the spherical array. However, when the temporal resolution of the measurement is high, the problem is significantly alleviated. The total spatial resolution of the measurement system is determined by the angular resolution of the spherical array of approximately 40° and the 33 ns delay resolution of the wideband channel sounder. Thus the spatial resolution intervals are truncated cones with an opening angle of 40° and length of 10 m. More closely spaced waves sum up at the receiver in a complex manner, which causes uncertainty in the estimated DoA. According to the fading analysis presented in [17], the average Rice factor of the amplitudes of the resolved multipath components is approximately 12 dB in urban environment, which means that they can be considered to be composed of one dominant wave with fair accuracy.

III. Measurement Environment

We carried out the measurements in an urban environment in the centre of Helsinki, Finland, in June 2000. We mounted the sector transmit antenna sequentially in two different base station sites. The sites were exactly the same as the two macrocell sites used in the directional measurements at the base station [10], there referred to as RX2 and RX3. For clarity, in this paper we will call the sites TX2 and TX3, respectively. The antenna heights from ground were 27 m (TX2) and 21 m (TX3). Site TX2 was at, and site TX3 above the rooftop level of the surrounding buildings. Photographs showing the views from both sites can be found in [10], together with detailed descriptions of the characteristic environmental features of both sites.

The spherical array at the receiver was mounted on a trolley at street level, with the centre of the array being at the height of 1.7 m, corresponding to the height of a normal mobile terminal. The total number of mobile terminal locations in which static measurements were made was 50 (32 for TX2, 18 for TX3). These locations are exactly the same as those used in the directional measurements at the base station, described in [10]. In addition, 11 continuous mobile routes were measured [13]. In the analysis presented in this paper we only use those routes that were measured in street canyons. The total length of these routes was 1830 m, and the total number of snapshots collected along the routes was 65'600. The trolley was pushed along sidewalks on the streets in the measurement area, and the TX–RX distance varied within 50...750 m. The measurement distance was limited by the sensitivity of the channel sounder, due to losses in the switching unit. Fig. 1 presents a map of the area showing the two transmitter sites, all static measurement locations, and the continuous mobile routes in street canyons. The street grid in the measurement area is fairly regular and the average street width is approximately 15 m. The height of most buildings is in the range of 20...30 m (see Fig. 1).

IV. Sample Results

We separately analysed data from the 50 static measurement locations, by plotting the total received power as the sum of the powers of the θ- and ϕ-polarised components at the mobile station in *azimuth-elevation, azimuth-delay,* and *elevation-delay* planes. We compared the results with those obtained from the measurements at the base station, and identified distinct propagation paths. In this section we will show a few sample results of the analysis, representing the typical propagation phenomena. Three of the four selected locations are the same as presented in [10], to enable the comparison of results at both ends of the propagation channel. The numbering of the locations is the same as used in [10], so that location RX5 (TX2) in this paper is the same as TX5 (RX2) in [10].

A. Mobile terminal location RX5 (TX2)

In our first example the mobile was located near the northeastern corner of an open square, only 180 m from the BS, behind a block of buildings. Fig. 2 presents a detailed map of the environment surrounding the mobile terminal, and the orientation of the co-ordinate system. Figs. 3 and 4 show the received power at the mobile station over the azimuth-elevation and azimuth-delay planes, respectively. In Fig. 3 the elevation angle increases from the centre towards the edges of the figure. The dashed line marks the horizontal plane, i.e. elevation of 0°. Similarly, in Fig. 4 the propagation delay increases from the centre towards the edges. The darker colours of the contour plots indicate higher received power. The colour scale is normalised to the maximum power in each graph.

The first multipath component arrived with a delay of 0.6 μs from direction (ϕ,θ) = (–95°, 25°), and it could be identified as the direct path from the TX direction, diffracted over the building roof (*Quasi-LOS*). The next component, which is the strongest one, was received at a delay of 0.7 μs, via a reflection from the metal roof next to the *White tower* (see Fig. 2), which had LOS to the BS site. In the BS measurement of the same mobile terminal location (see Figs. 13 and 14 in [10]), we erroneously interpreted this reflection to have originated from the *White Tower*, but from the mobile end the difference between the azimuth directions is clear (*White Tower:* –40°, *metal roof:* –50°). Other components , which initially propagate over the rooftop, are the reflection from the *Theatre tower*, and secondary reflections from the *Theatre Building*. The rest of the signal components originally propagate along *Kaisaniemenkatu* street canyon. The first of

them is visible in the direction of the street aperture, while the rest are multiple reflections from the *Railway Station* and other buildings on the sides of the open square. By combining the results with the measurement at the BS end of the channel (see Figs. 13 and 14 in [10]), we can completely resolve and identify the dominant propagation paths to this mobile terminal location. The schematic diagram in Fig. 5 describes how the secondary signal sources seen by the base station are linked to those seen by the mobile station. Double reflections/diffractions are observed via *Theatre Tower* and street canyon.

B. Mobile terminal location RX18 (TX2)

In the second example the mobile was located in the southeastern corner of the open square, close to the aperture of the street canyon leading to the BS. Fig. 6 presents a detailed map of the environment surrounding the mobile terminal, and Figs. 7 and 8 show the received power at the mobile station over the azimuth-elevation and azimuth-delay planes, respectively. The strongest signal components in this location were received at rather low elevation angles from the direction of the street canyon (ϕ = [−12°…−22°]), as could be expected. Reflections with short delays are observed from the corner of *Ateneum* building ($\phi \approx 75°$) as well as the building wall at the right-hand side. In addition, longer-delayed components reflected from the opposite side of the open square were identified. The interesting special aspect concerning the signals received in this location is the strong multipath component received at a small excess delay from an azimuth of 20°, one of them at an elevation angle of approximately 60°. Since there are no buildings close to the mobile in this direction, we first suspected a measurement error. However, we visited the measurement area once again and found that the source of these multipath components with high elevation angles and short delays was a high lamp post next to the location of the mobile terminal, see Fig. 6. This example demonstrates that even small objects, not only buildings, affect the propagation in urban environments.

C. Mobile terminal location RX28 (TX2)

Fig. 9 presents a detailed map of the environment surrounding the mobile terminal in location RX28 (TX2), situated in the street canyon of *Aleksanterinkatu*. In [10] we presented results from measurements at the BS end of the link to this location (see Figs. 15 and 16 in [10]). We then observed that the strongest multipath component was received with an excess delay of 1.4 μs, from the direction of the highest building in the surroundings (*Hotel Torni*). Fig. 10 shows a photograph taken from this building towards the measurement area. Site TX2, and *Stockmann* and *Makkaratalo* buildings are marked in the photograph. As can be observed in Fig. 10 the metal roof of *Stockmann* building rises higher than the neighbouring *Makkaratalo* building. There is a LOS from site TX2 to the *Stockmann* roof as well as to the building with *Glass wall* (see Fig. 9). Figs. 11…13 show the received power at the mobile station over azimuth-elevation, azimuth-delay, and elevation-delay planes, respectively. The first multipath component is received through a reflection from the metal roof of *Stockmann* building. Almost simultaneously a large number of multipath components can be observed from all azimuth directions except for the range +90°…+150°, where the closest buildings are more than 100 m away (*street scattering & multiple reflections in street canyon*). The components from high elevation angles and azimuths of +20° and –40° are the result of secondary scattering from the roof of the *Stockmann* building and then from the wall of *Makkaratalo* building (the mobile was situated on the sidewalk only a couple of meters from the wall). The components having the longest delays were reflected from the *Glass wall* (azimuth range +90°…+120°) and *Hotel Torni* (azimuth +120°) after propagating over the *Makkaratalo* building. The effect of the coupling to the street level after reflection from the high-rising roof is very clear in the elevation-delay profile in Fig. 13, where the highest components have shortest delays. Based on the mobile station measurements it can be concluded that the interpretation of the BS measurements was partly in error. The components that were actually reflected from the *Glass wall* after propagating over the *Makkaratalo* building were then assumed to have propagated via *Keskuskatu* street canyon and therefore visible in the azimuth direction of *Makkaratalo* building. The erroneous interpretation was due to poor measurement resolution in the elevation plane, which made it difficult to distinguish separate distant secondary sources.

The foregoing example demonstrates an important finding. Energy that arrives from directions roughly perpendicular to street can be reflected or diffracted down to street level by buildings on the opposite side of the street from the direction to the source that are higher than those that line the side of the street in the direction of the source. This was the situation in most measurement cases where propagation over rooftops played a significant role. In many of these cases the coupling happened through backward diffraction from the building roof-edge (or scattering from objects near the rooftop level) on the opposite side of the street, having LOS to the base station.

D. Mobile terminal location RX3 (TX3)

The last example is the mobile terminal location RX3 (TX3). Fig. 14 presents a detailed map of the surroundings of this location, and Figs. 15 and 16 show the received power at the mobile station over the azimuth-elevation and azimuth-delay planes, respectively. During measurements at the BS [10] we noticed that most of the power propagates via two streets: *Rauhankatu* and *Kirkkokatu* (see Fig. 14). Also components propagating over the rooftop of *BOF*-building and reflections from the high-rising cupola of the Lutheran cathedral (*Church*) were observed at the BS. The measurements at the mobile station are consistent with these results. By looking at Figs. 15 and 16 it is clear that the propagation along *Rauhankatu* street canyon dominates. Most multipath signals were received from azimuths between –50°

and +50°. These correspond to the buildings to the north of the mobile terminal location. The reflection from the *Church* cupola was found to arrive from an azimuth of +135°, with an elevation angle between 25° and 30° above horizon.

The most interesting observation is that no short-delayed multipath components are received from the direction of the BS ($\phi \approx 80°$), see Fig. 16. Instead, components with high elevation angles ($\theta \approx 50°$) are found on the opposite side, around azimuths between −50° and −140°. These directions correspond to the top corners of the building closest to the mobile terminal location (see Fig. 15). The interpretation of this result is that these components were originally propagated over the *BOF*-building, but received at the mobile via diffraction from the opposite building roof-edge (or scattering from objects near the rooftop level), which has LOS to the BS. The phenomenon is exactly the same that was observed for mobile terminal location RX28 (TX2), in Sec. IV.C. The result also reveals the requirement to look into the propagation channel from both ends of the link, to make the correct conclusions about the actual propagation paths.

V. Consistency of Propagation Paths

In order to investigate the consistency of the resolved propagation paths, and thus the reliability of the static measurement results presented in the previous section, we also performed measurements along continuous routes.

We present two examples showing the large-scale variation of the power received over certain propagation paths when the mobile terminal moved continuously along one of the measurement routes. Both the presented examples are from a single measurement route, at a distance of approximately 500 m from the base station. Fig. 17 shows the local surroundings and geometry of the route. The marker numbers correspond to snapshot counter values. Measurement snapshots were taken at a period of approximately 2.8 cm ($\lambda/5$) along the route, i.e. 1000 snapshots corresponds to a 28 m movement of the mobile terminal.

A. An Over-Rooftop Propagation Path

The first example shows the properties of wave interaction from a metal building roof having LOS to the base station. The building between the base and mobile stations is clearly lower than the building on the opposite side of the street. The upper-most graph of Fig. 18 presents the θ- (VP) and ϕ- (HP) polarised power received from the direction of the metal roof (±10° azimuth window), at elevation angles higher than 25°. The power has been averaged with a sliding window of 20 snapshots, i.e. app. 4 wavelengths. The figure shows significant variation of power carried by this propagation path. Between snapshots #5250 and #6150 the power in this direction is clearly higher when compared to the rest of the route, at maximum the difference is of the order of 20 dB. The snapshot range corresponds to the part of the route, where the roof was at an azimuth angle of 95° relative to the mobile terminal, i.e. at an offset of 5° compared to the normal of the building wall (see Fig. 17). The angles fit well to the geometry of the backward diffraction, since the angle of incidence of the plane wave coming from the base station is −5° off the normal of the wall. Vertical polarisation dominates the signal received from the roof. The cross polarisation power ratio (XPR) of the signals received over the propagation path and averaged over the measurement route is 9.7 dB.

The lowest graph in Fig. 18 shows the total received power along the same route. It can be seen that the highest value of the received power along the route occurred when the mobile terminal passed by the metal roof. In the range between snapshots #5400 and #5850 the average portion of power propagating via the roof is 69 % of the total received power (in average 45 % between snapshots #5250 and #6150). Thus this propagation path clearly dominated at this part of the route. The XPR averaged over the measurement route was 8.2 dB, which is close to the average over all mobile station measurements (8.6 dB [13]), and the average XPR measured at the base station (8.0 dB [18]).

B. A Street-Canyon Propagation Path

The other propagation path that was investigated is believed to have involved diffraction from the building block corner marked in Fig. 17. The waves that travelled along the street that approaches the intersection from the direction of the base station illuminated the street crossing, and the mobile terminal received power from the direction of the block corner. The centre plot of Fig. 18 presents the θ- (VP) and ϕ- (HP) polarised power received from the direction of the block corner (±10° azimuth window), at elevation angles above horizontal plane. It can be seen that this propagation path is clearly more stable than the one of the previous example. The VP power varies within –80... –90 dBm for most of the route. There is a trend of increasing power towards the end of the route, which is explained by the fact that as time progressed, the mobile terminal came closer to the street crossing. Vertical polarisation dominated on this propagation path: the XPR averaged over the route was 10.8 dB.

VI. Angular Power Distribution and Excess Delay

We computed the estimates of the Azimuth Delay Power Profile (ADPP) and Elevation Delay Power Profile (EDPP) over all data measured along continuous routes in street canyons. The routes are shown in Fig. 1. Measurements were performed in such a way that azimuth angles 0° and 180° were parallel to the street canyon. The mobile moving direction was 0° in azimuth.

The details of computing the angle-delay power profiles based on the angular resolved impulse response estimates are presented in [17]. First the angle-delay planes were divided into equally spaced bins and for each snapshot the powers of all multipath components corresponding to each bin were summed. The resulting matrix was normalised by the total

incident power of each snapshot, to compensate for large-scale variations of the received power. Finally the ADPP and EDPP were computed by averaging over all recorded snapshots.

Figs. 19 and 20 present the EDPP averaged over all street canyon routes for the excess delay and absolute delay, respectively. The shape of the EDPP for excess delay demonstrates how the energy propagating above rooftops is coupled to street level with short excess delays. Propagation along street canyons dominates for excess delays larger than 1 μs, which can be seen as low elevation angles. The maximum of the average EDPP for excess delay is found at an elevation angle of 7° and an excess delay of 0.3 μs. The average EDPP for the absolute delay has a different shape. Propagation over building rooftops is strongest inside the absolute delay range between 1 μs and 2.5 μs (BS-MS distance of 300...750 m). Propagation via street canyons dominates for delays outside this range. The measurement range explains the upper limit of the delay range: the longest distance between BS and MS in the measurements was approximately 750 m, corresponding to a propagation delay of 2.5 μs.

The correlation between azimuth angle and excess delay can be seen in Fig. 21. For short excess delays the power spreads almost equally in all azimuth directions, but at an excess delay of approximately 0.4 μs certain directions begin to dominate. The longest delays were found in the directions of the street canyon (0°, 180°), but also the effect of intersecting streets can be seen as longer delays around azimuth angles of ±90°. Similar behaviour has been observed before by Kuchar et al. in a city having considerably different street orientations and construction characteristics [8], even with the same breakpoint value of 0.4 μs.

VII. Conclusions

This paper reports the application of a measurement technique based on use of a spherical antenna array and a wideband channel sounder to characterise the influence on propagation of the 3-D environment surrounding a mobile terminal in an urban environment. By combining the results of directional radio channel measurements at both ends of the link we were able to identify precisely the last wave interaction points before the wave reaches the base and mobile stations, and to investigate the relative strength of various reflecting, scattering, and diffracting contributions.

In [10] we concluded that propagation over building roofs typically occurs via buildings that rise higher than the average rooftop level. Based on analysing data measured at the mobile terminal we conclude that even small differences in building heights are in connection with the propagation of waves which arrive from over rooftops, then impinge on the top edges of building walls and are diffracted into street canyons. In most cases the signal components with high elevation angles were due to reflections from building roofs with LOS to the base station. As already observed in [10], the components diffracted directly over the rooftop from the direction of the BS were mostly weak, and in many cases they did not exist at all. Instead, coupling of energy to street level typically happened via the building roof opposite to the direction of the BS. This finding indicates that building height is an important parameter in site-specific deterministic propagation models, such as those based on ray tracing.

The results prove that the radio environment at the mobile terminal is different from that at the base station. In the urban macrocell environment the spread of energy in both the azimuth and elevation angle domains is significantly larger at the mobile terminal. In some cases even the power scattered from lampposts could be identified. Thus for a small handheld terminal antenna having low directivity, the contribution of high-elevation multipath components is significant.

We tracked the individual propagation paths over a continuous route, and demonstrated how the relative powers of the paths vary when the terminal moves in the environment. The dominant propagation mechanism – e.g. propagation over rooftops or via street canyons – may change entirely along the route, resulting also in considerable variation of received power within relatively short distances. These findings support the concept of local regions of consistency in the parameters of the set of waves that arrive at a mobile terminal [19,20,21] and show the usefulness of our measurement approach to determine such regions.

The results concerning the distribution of angles from which waves arrive at a mobile terminal in a microcellular environment are consistent with the findings in [8]. For short excess delays signal components are incident from all directions in azimuth, and from a wide range of elevation angles due to coupling from above rooftops. For large excess delays propagation via street canyons dominates, which can be seen by the concentration of energy in low elevation angles, and in azimuth sectors corresponding to the street directions.

In the future, when antenna arrays are introduced at the base and mobile stations of cellular networks, accurate modelling of the spatial radio channel will become crucial. Based on the results presented in this paper it is evident that deterministic site-specific propagation modelling in urban macrocells requires accurate 3-D ray tracing, with detailed information of building heights and materials. The measured double-directional radio channel data can be utilised in the verification and evaluation of existing ray tracing tools. Double-directional channel measurements will also pave the way for site-specific radio network deployment [22]. This technique will make possible considerable savings in transmitted power and reduction in intra-system interference by making it possible to transmit only in directions where one can be sure that the signal will be actually received and will harm other receivers in the cell least.

ACKNOWLEDGMENT

The authors wish to thank Martti Toikka, Lasse Vuokko, Pasi Suvikunnas, and Eero Rinne for their help in carrying out the radio channel measurements. Also the anonymous reviewers of the manuscript are acknowledged for their valuable comments.

REFERENCES

[1] A. J. Paulraj and C. B. Papadias, "Space-time processing for wireless communications, improving capacity, coverage, and quality in wireless networks by exploiting the spatial dimension," *IEEE Signal Processing Magazine,* vol. 14, no. 2, pp. 49-83, November 1997.

[2] G. J. Foschini and M. J. Gans, "On limits of wireless communication in a fading environment when using multiple antennas," *Wireless Personal Communications*, vol. 6, no. 3, pp. 311–335, March 1998.

[3] C. B. Dietrich, Jr., W. L. Stutzman, K. Byung-Ki, K. Dietze, "Smart antennas in wireless communications: base station diversity and handset beamforming," *IEEE Antennas and Propagation Magazine,* vol. 42, no. 5, pp. 142-151, October 2000.

[4] R. B. Ertel, P. Cardieri, K. W. Sowerby, T. S. Rappaport, and J. H. Reed, "Overview of spatial channel models for antenna array communications systems," *IEEE Personal Communications,* vol. 5, no. 1, pp. 10-22, February 1998.

[5] Luis M. Correia (ed.), *Wireless Flexible Personalised Communications, COST 259: European Co-operation in Mobile Radio Research*. Chichester: Wiley, 2001, 512 p.

[6] M. Steinbauer, D. Hampicke, G. Sommerkorn, A. Schneider, A. F. Molisch, R. Thoma, and E. Bonek, "Array measurement of the double-directional mobile radio channel," *Proc. 51st IEEE Vehicular Technology Conference (VTC 2000 Spring),* Tokyo, Japan, May 15-18, 2000, pp. 1656-1662.

[7] J. Fuhl, J.-P. Rossi, and E. Bonek, "High-Resolution 3-D Direction-of-Arrival Determination for Urban Mobile Radio," *IEEE Trans. Antennas and Propagation,* vol. 45, no. 4, pp. 672-682, April 1997.

[8] A. Kuchar, J.-P. Rossi, and E. Bonek, "Directional Macro-Cell Channel Characterization from Urban Measurements," *IEEE Trans. Antennas and Propagation,* vol. 48, no. 2, pp. 137-146, February 2000.

[9] H. Laitinen, K. Kalliola, and P. Vainikainen, "Angular Signal Distribution and Cross-Polarization Power Ratio Seen by a Mobile Receiver at 2.15 GHz," *Proc. Millennium Conference on Antennas & Propagation (AP2000),* Davos, Switzerland, April 9-14, 2000, CD-ROM SP-444 (ISBN 92-9092-776-3), paper p1133.pdf.

[10] J. Laurila, K. Kalliola, M. Toeltsch, K. Hugl, P. Vainikainen, and E. Bonek, "Wideband 3-D Characterization of Mobile Radio Channels in Urban Environment", IEEE Trans. Antennas and Propagation, vol. 50, no. 1, pp. 1-11, January 2002.

[11] H. L. Bertoni, *Radio Propagation for Modern Wireless Systems*. New Jersey: Prentice Hall PTR, 2000, 258 p.

[12] N. Blaunstein, *Radio Propagation in Cellular Networks*. Boston: Artech House, 2000, 386 p.

[13] K. Kalliola, H. Laitinen, K. Sulonen, L. Vuokko, and P. Vainikainen, "Directional Radio Channel Measurements at Mobile Station in Different Radio Environments at 2.15 GHz," *Proc. 4th European Personal Mobile Communications Conference (EPMCC 2001)*, Vienna, Austria, February 20-22, 2001, CD-ROM ÖVE 27 (ISBN 3-85133-023-4), pap113.pdf.

[14] K. Kalliola, H. Laitinen, L.I. Vaskelainen, and P. Vainikainen, "Real-time 3D Spatial-Temporal Dual-polarised Measurement of Wideband Radio Channel at Mobile Station," *IEEE Trans. Instrumentation and Measurement*, vol. 49, no. 2, pp. 439-448, April 2000.

[15] J.-P. Rossi, J.-P. Barbot, and A.J. Levy, "Theory and Measurement of the Angle of Arrival and Time Delay of UHF Radiowaves Using a Ring Array," *IEEE Trans. Antennas and Propagation, vol. 45, no. 5,* pp. 876-884, May 1997.

[16] J. Kivinen, T. Korhonen, P. Aikio, R. Gruber, P. Vainikainen, S.-G. Häggman, "Wideband Radio Channel Measurement System at 2 GHz," *IEEE Trans. Instrumentation and Measurement*, vol. 48, no. 1, pp. 39-44, February 1999.

[17] K. Kalliola, *Experimental analysis of multidimensional radio channels*. Doctoral dissertation, Helsinki University of Technology, February 2002, Finland. Available: http://lib.hut.fi/Diss/2002/isbn951225705X/.

[18] M. Toeltsch, J. Laurila, A.F. Molisch, K. Kalliola, P. Vainikainen, and E. Bonek, "Spatial Characterization of Urban Mobile Radio Channels," *Proc. 53rd IEEE Vehicular Technology Conference (VTC 2001-Spring)*, Rhodes, Greece, May 6-9, 2001.

[19] M. Steinbauer, *The Radio Propagation Channel – A Non-Directional, Directional, and Double-Directional Point-of-View*. PhD Dissertation, Technische Universitaet Wien, November 2001, Vienna, Austria. Available: http://www.nt.tuwien.ac.at/mobile/theses_finished/.

[20] A. Gehring, M. Steinbauer, I. Gaspard, and M. Grigat, "Empirical channel stationarity in urban environments," *Proc. 4th European Personal Mobile Communications Conference (EPMCC 2001)*, Vienna, Austria, February 20-22, 2001, CD-ROM ÖVE 27 (ISBN 3-85133-023-4), pap20.pdf.

[21] R. J. C. Bultitude, T. J. Willink, M. H.A. J. Herben, and G. Brussaard, "Detection of changes in the spectra of measured CW mobile radio data for space wave modelling applications," *Proc. Queens University Bienniel Symposium on Communications*, Kingston, Canada, May 28-31, 2000, pp. 90-94.

[22] E. Bonek and M. Steinbauer, "Double-Directional Channel Measurements," *Proc. 11th Int. Conf. Antennas and Propagation (ICAP 2001)*, Manchester, UK, April 17-22, 2001, IEE Publ. No. 480, pp.226-230.

Kimmo Kalliola was born in Helsinki, Finland, in 1972. He received the M. Sc., Lic. Sc., and D.Sc. (Tech.) degrees from Helsinki University of Technology (HUT) in 1997, 2000, and 2002, respectively. In his doctoral thesis he investigated methods for multidimensional radio channel measurements. In 1997-2001 he was with the Radio Laboratory of HUT, working as a research engineer in the field of radio propagation measurements for mobile communications. Since 1999 he has been working as research engineer and most recently as assistant research manager at Nokia Research Center (Radio Communications Laboratory), Helsinki, Finland. His current research interests are in radio propagation measurements and modeling for wireless communication systems. He is the author or co-author of 5 reviewed journal articles and 13 international conference papers.

Heikki Laitinen was born in Helsinki, Finland, in 1972. He received the Master of Science in Technology degree in 1999 from Helsinki University of Technology. Since 1998 he has been with the Technical Research Centre of Finland (VTT), where he is currently working as a Research Scientist. His research interests include radiowave propagation modeling and location techniques.

Pertti Vainikainen (M'91) was born in Helsinki, Finland in 1957. He received the degree of Master of Science in Technology, Licentiate of Science in Technology and Doctor of Science in Technology from Helsinki University of Technology (HUT) in 1982, 1989 and 1991, respectively. He worked at the Radio Laboratory of HUT from 1981 to 1992 mainly as a teaching assistant and researcher. From 1992 to 1993 he was Acting Professor of Radio Engineering, since 1993 Associate Professor of Radio Engineering and since 1998 Professor in Radio Engineering, all at the Radio Laboratory of HUT. In 1993-97 he was the director of the Institute of Radio Communications (IRC) of HUT. His main fields of interest are antennas and propagation in radio communications and industrial measurement applications of radio waves. He is the author or co-author of 3 books and over 110 refereed international journal or conference publications and the holder of 4 patents.

Martin Toeltsch (S'00) received the Dipl.-Ing. degree (M.S.) in communications engineering and the Dr.Tech. degree from the Technische Universität Wien, Vienna, Austria (TU-Wien), in 1998 and 2002, respectively. In his doctoral thesis, he investigated high-resolution evaluations of directionally resolved radio channel measurements. From 1992 to 1998 he worked in the field of signal and image processing for medical applications.

From 1998 to 2002 he was a member of the Mobile Communications Group at the Institut für Nachrichten- und Hochfrequenztechnik (INTHF), TU-Wien. His research focused on OFDM and radio channel measurements, as well as propagation and channel modeling.

In 2002 he founded the SYMENA company where he developes smart antenna radio network planning and optimization tools.

Juha Laurila was born 1970 in Korpilahti, Finland. He received the M.Sc. (E.E.) degree from the Helsinki University of Technology, Finland (Institute of Radio Communications) in 1995 and the Dr.Tech. degree from the Vienna University of Technology, Austria (Institut fuer Nachrichtentechnik und Hochfrequenztechnik) in 2000. In his doctoral thesis he investigated semi-blind algorithms for mobile communications concentrating on the reception with multiple antennas at the base station. In 1995-96 he was with the Helsinki University of Technology and from 1996 to 2000 with the Vienna University of Technology, working as research engineer at both universities. Since 2000 he has been working as senior research engineer and most recently as research manager at Nokia Research Center (Radio Communications Laboratory) Helsinki, Finland. His current research activities are related to the utilisation of multiple antenna techniques in cellular systems. J. Laurila has authored or co-authored one book chapter and some 30 international reviewed journal and conference publications. He holds one patent and several applications are pending.

Ernst Bonek (M'73–SM'85) was born in Vienna, Austria, in 1942. He received the Dipl.Ing. and Dr.techn. degrees (with highest honors) from the Technische Universität Wien (TU Wien). In 1984, he was appointed Full Professor of Radio Frequency Engineering at the TU Wien. His field of interest is mobile communications at large. Recent contributions concern smart antennas, the characterization of mobile radio channels, and advanced antennas and receiver designs. Altogether, he authored or co-authored some 170 journal and conference publications. He holds several patents on mobile radio technology. He co-authored the book "Data Transmission over GSM and UMTS" by Springer Verlag, and co-edited "Technology Advances of UMTS" by Hermes Scientific Publications.

From 1985 to 1990, he served the IEEE Austria Section as a Chairman. From 1991 to 1994 he was a council member of the Austrian Science Fund, acting as speaker for engineering sciences. From 1996 to 1999 he served on the Board of Directors of the reorganized Post and Telekom Austria. He participated in the European research initiative COST 259 as chairman of the working group on Antennas and Propagation, and continues to serve in this position in COST 273. He is the initiator of ftw (Forschungszentrum Telekommunikation Wien), a public-private partnership for telecommunications research in Vienna, Austria.

List of figures:

Figures:

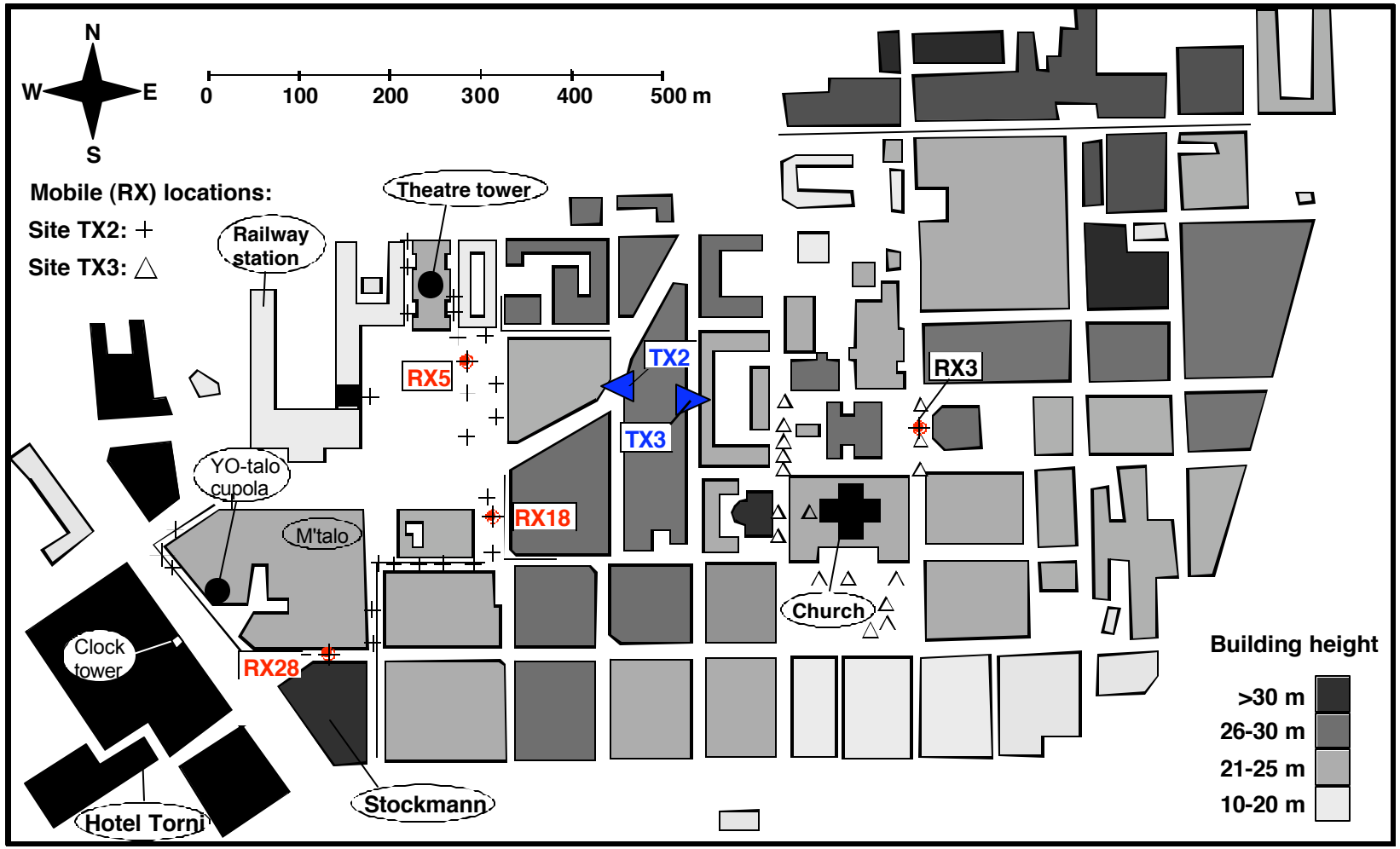

Figure 1. Measurement area in the centre of Helsinki (++, ΔΔ receiver positions, —— continuous mobile route).

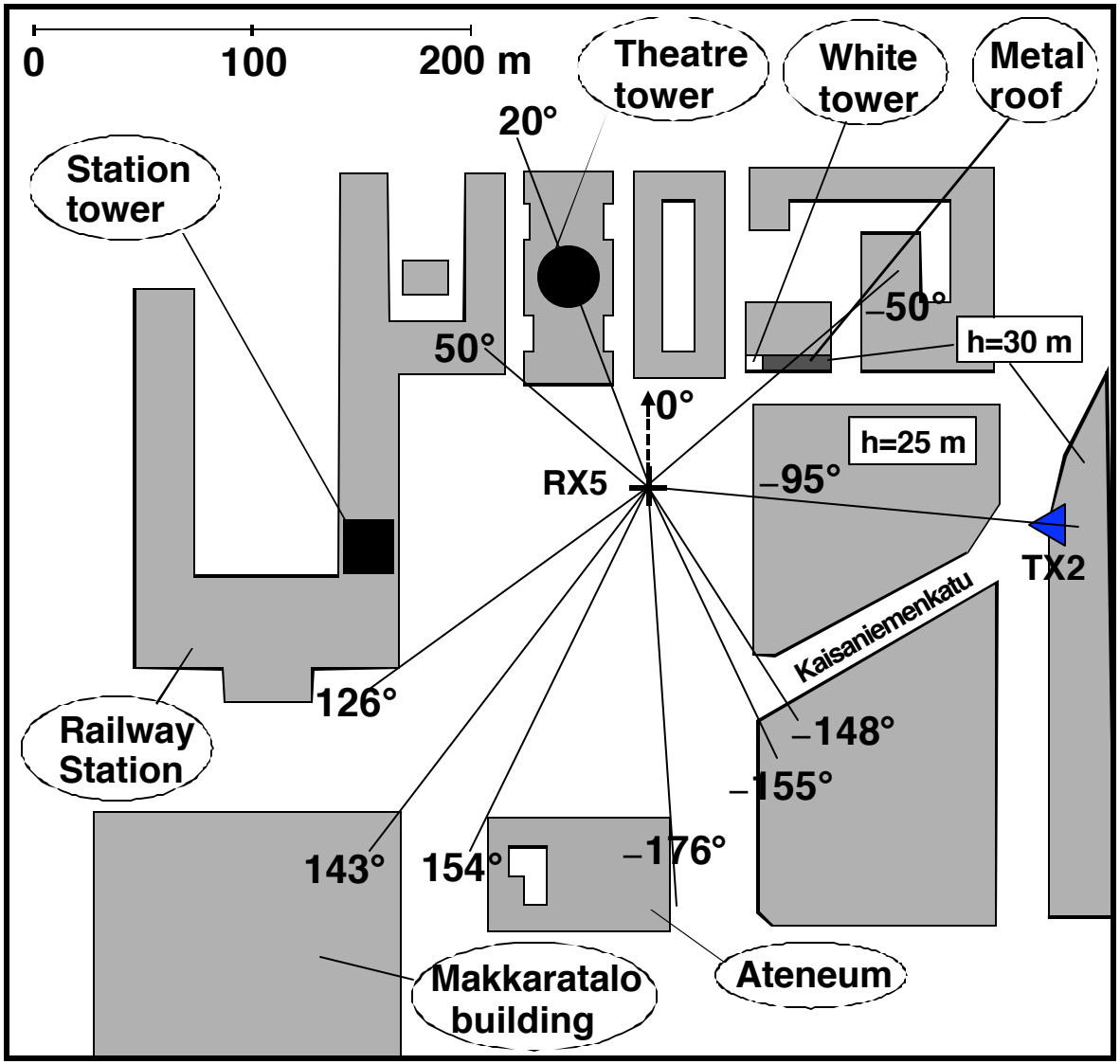

Figure 2. RX5 (TX2): Detailed map.

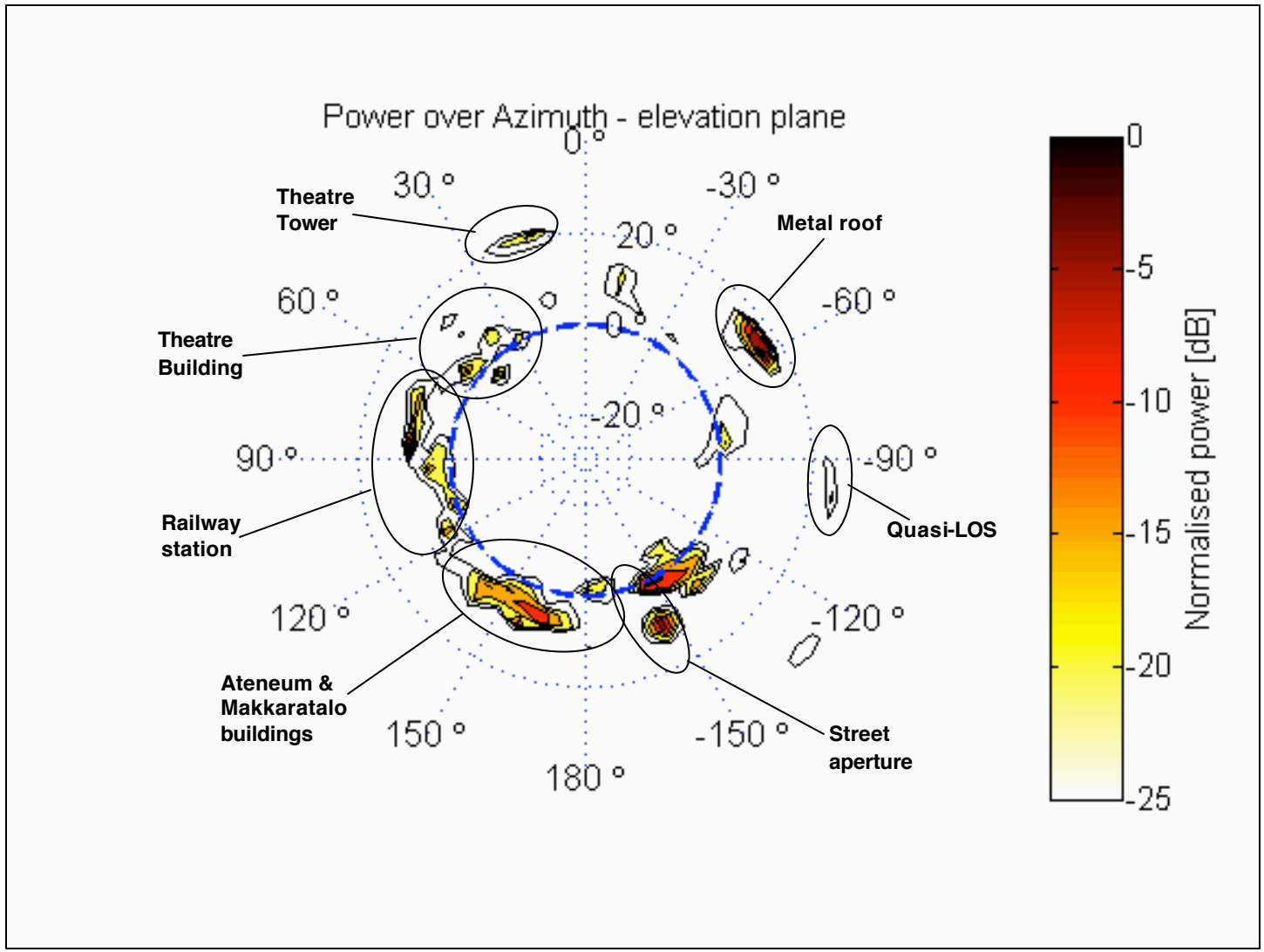

Figure 3. RX5 (TX2): Azimuth -elevation plane at mobile station.

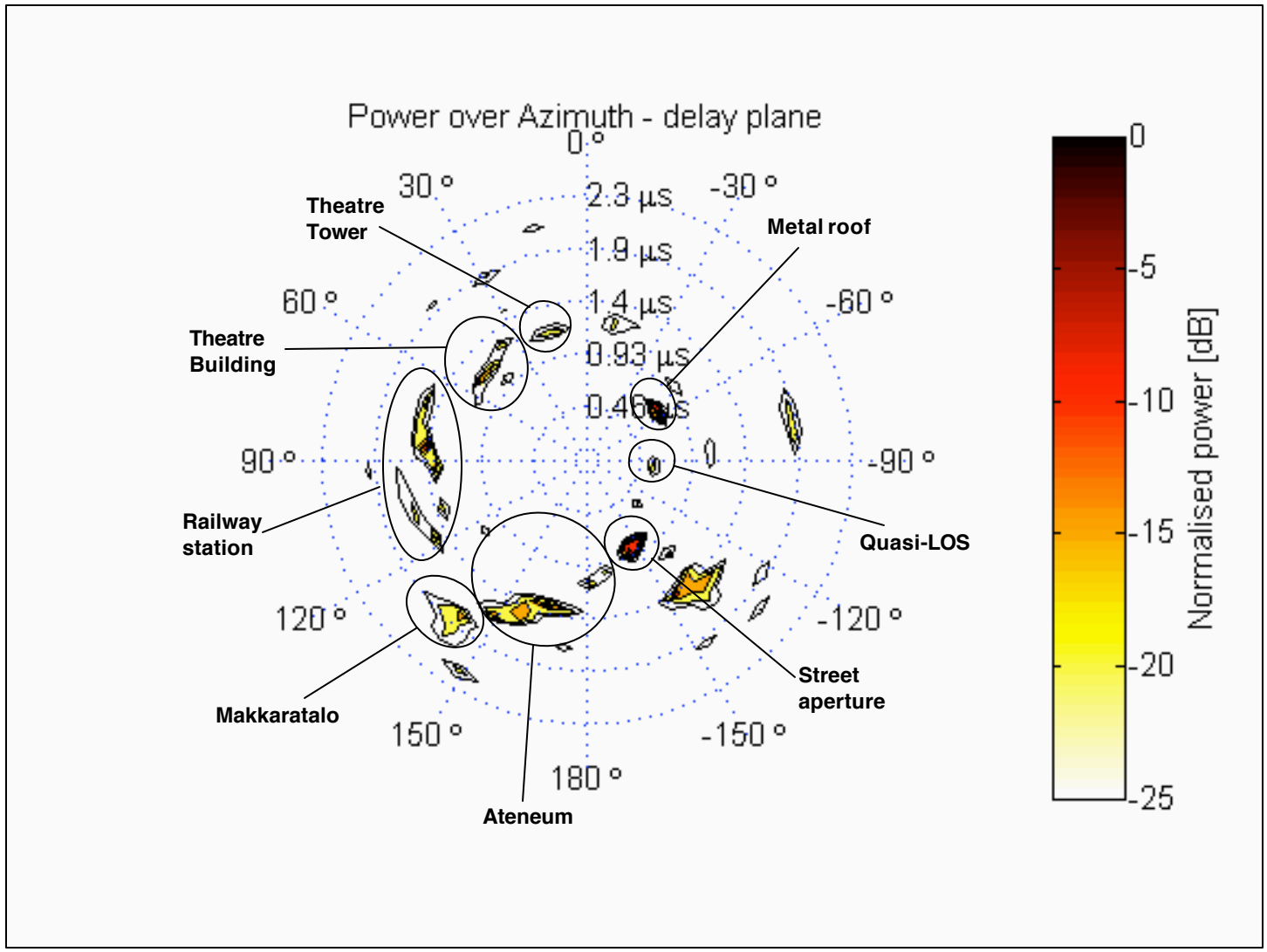

Figure 4. RX5 (TX2): Azimuth - delay plane at mobile station.

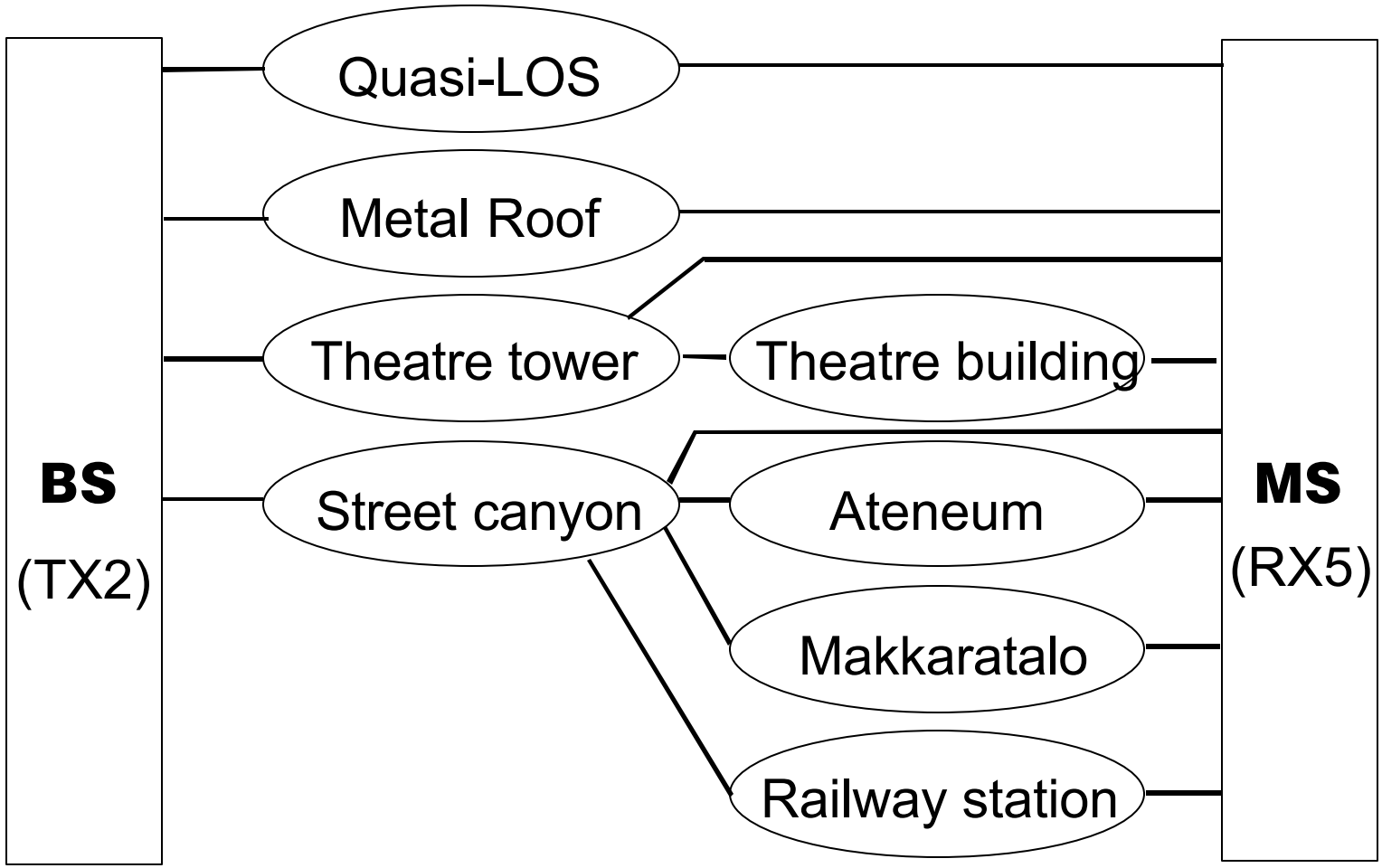

Figure 5. Block diagram of double-directional radio channel between TX2...RX5.

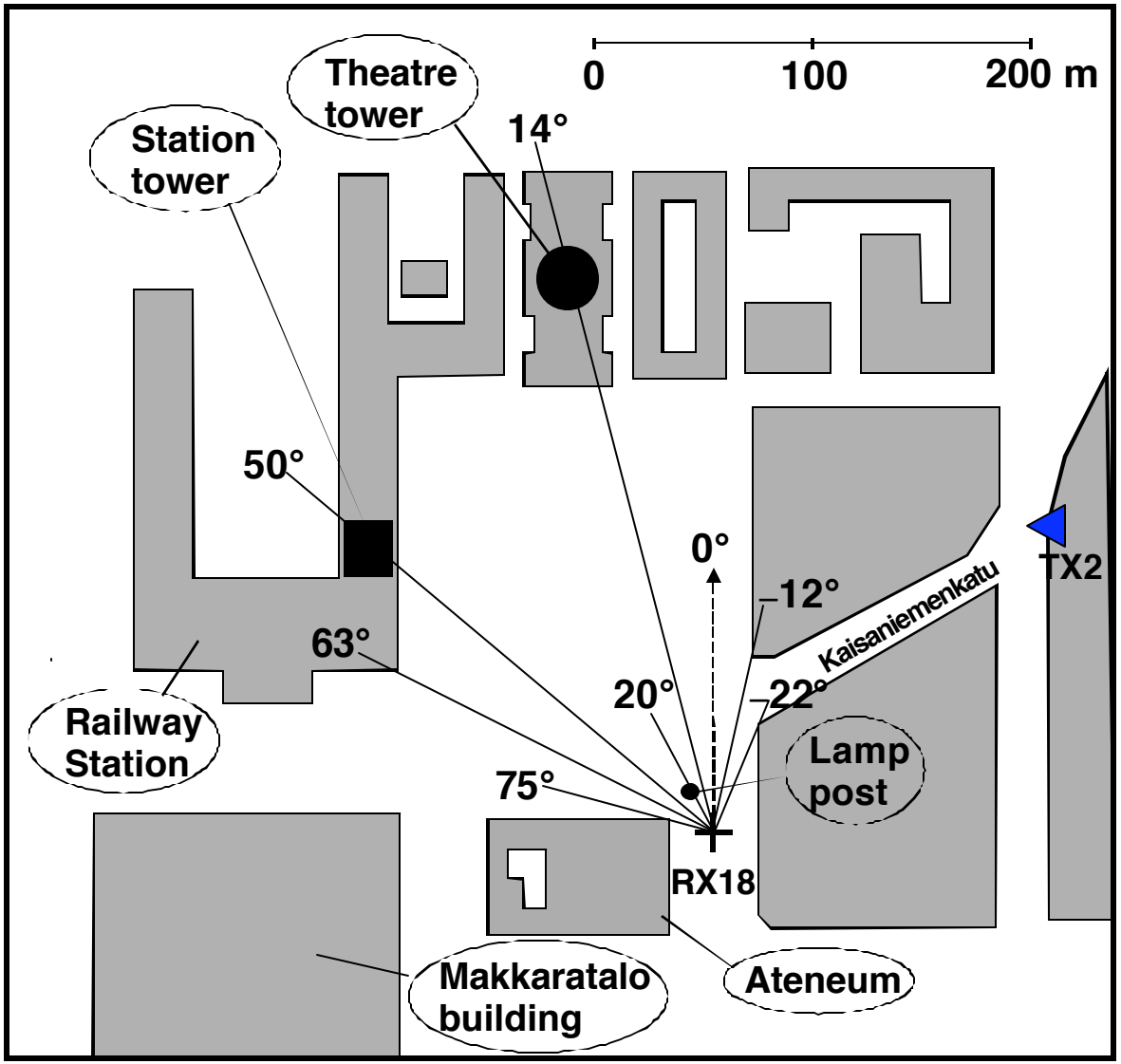

Figure 6. RX18 (TX2): Detailed map.

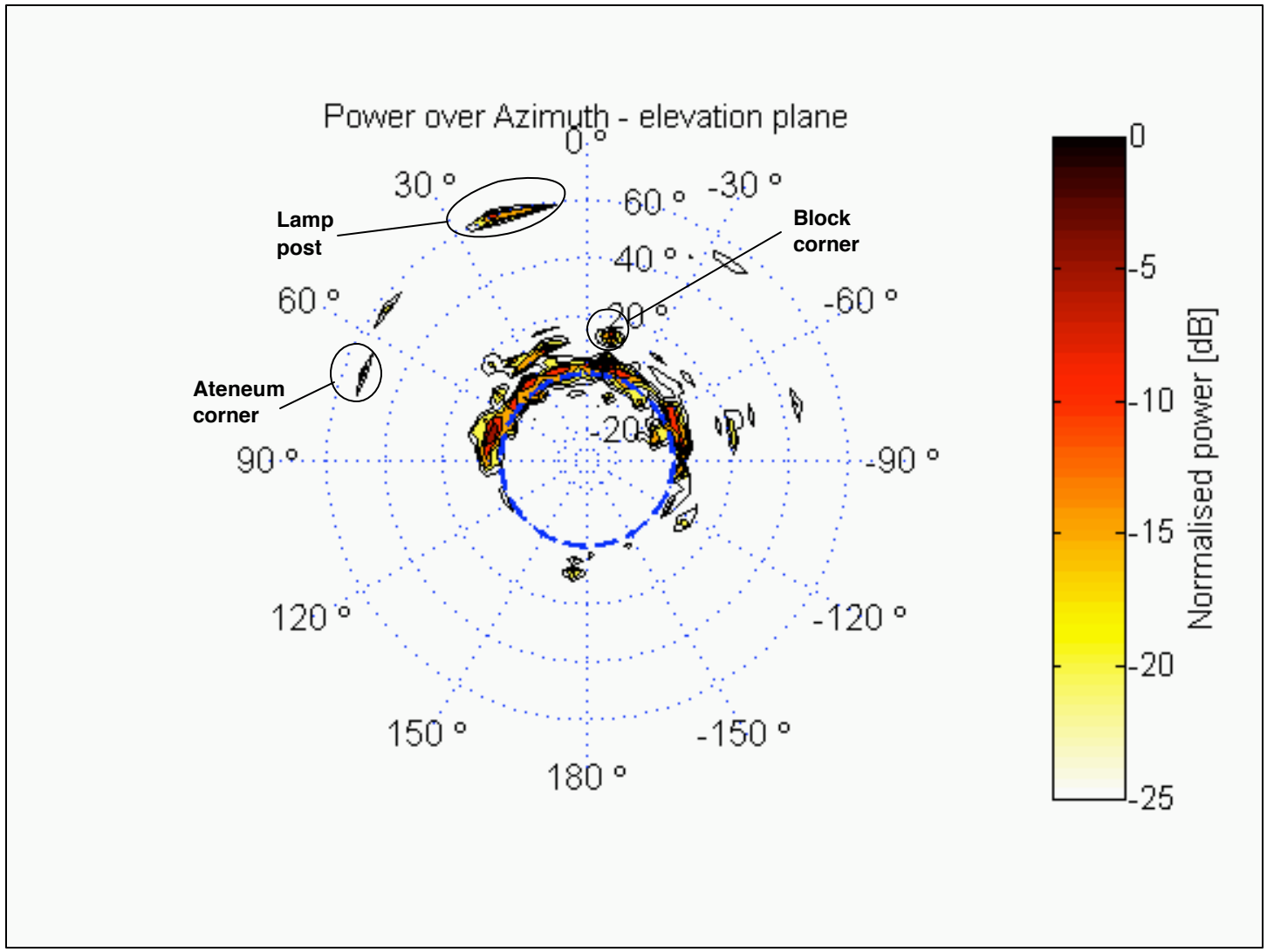

Figure 7. RX18 (TX2): Azimuth-elevation plane at mobile station.

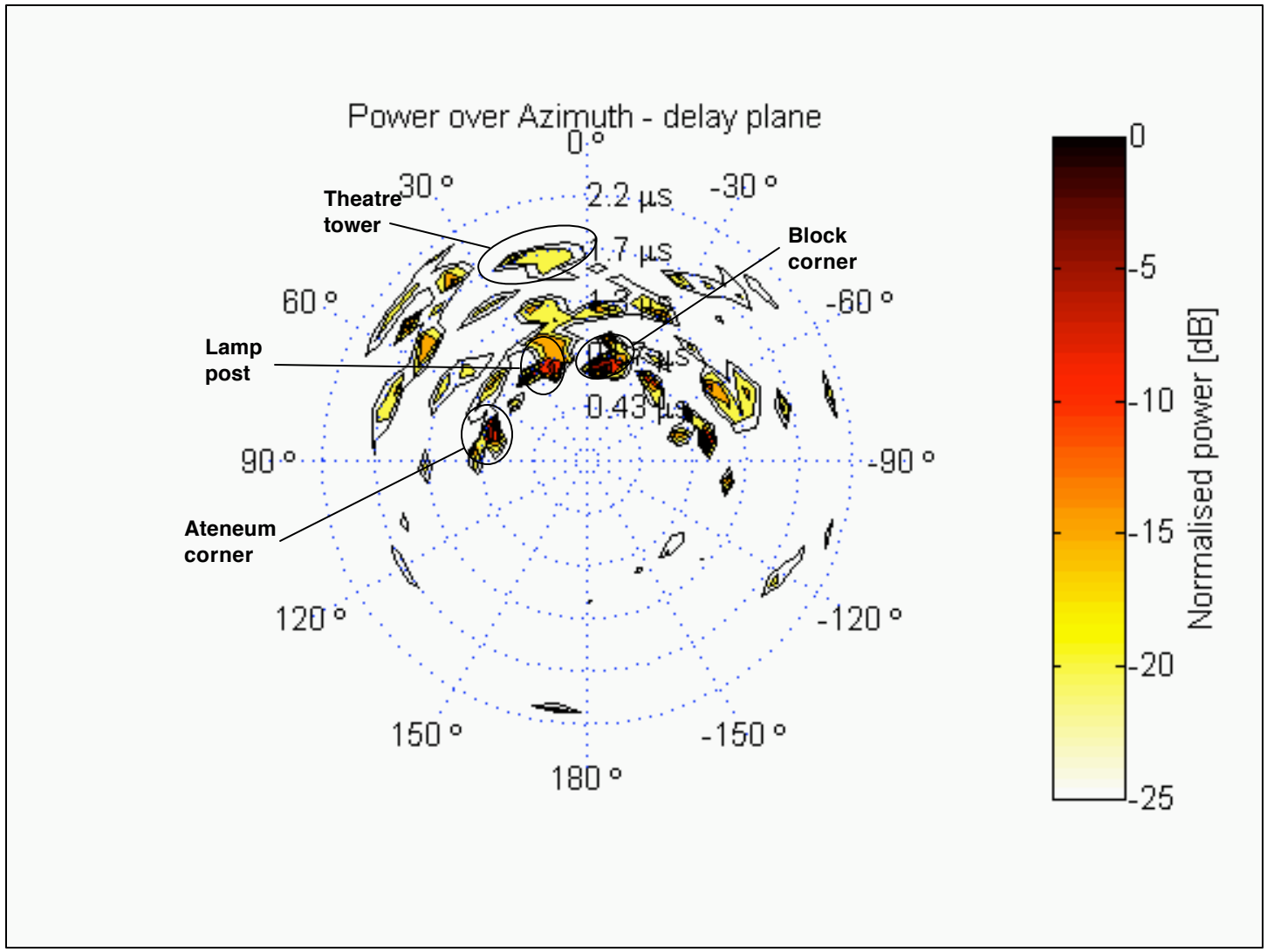

Figure 8. RX18 (TX2): Azimuth-delay plane at mobile station.

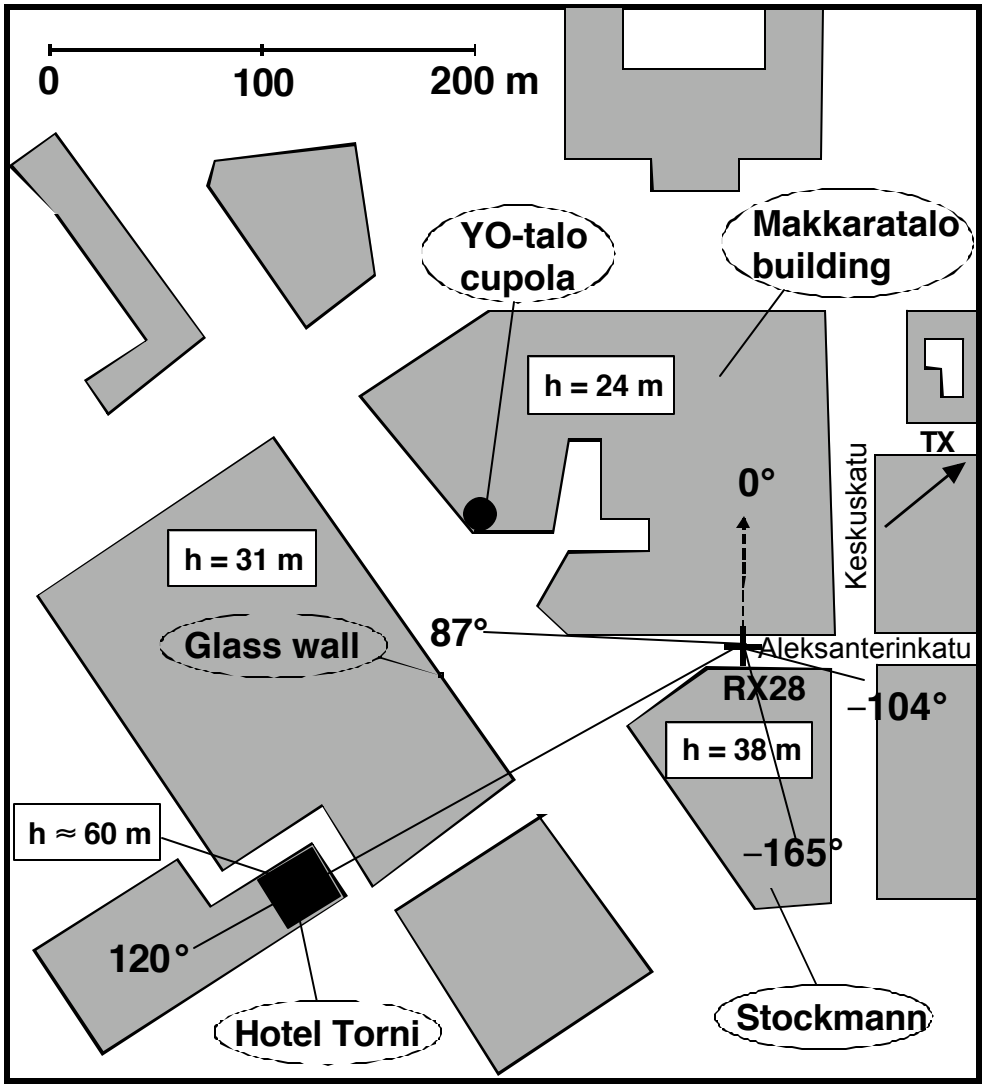

Figure 9. RX28 (TX2): Detailed map.

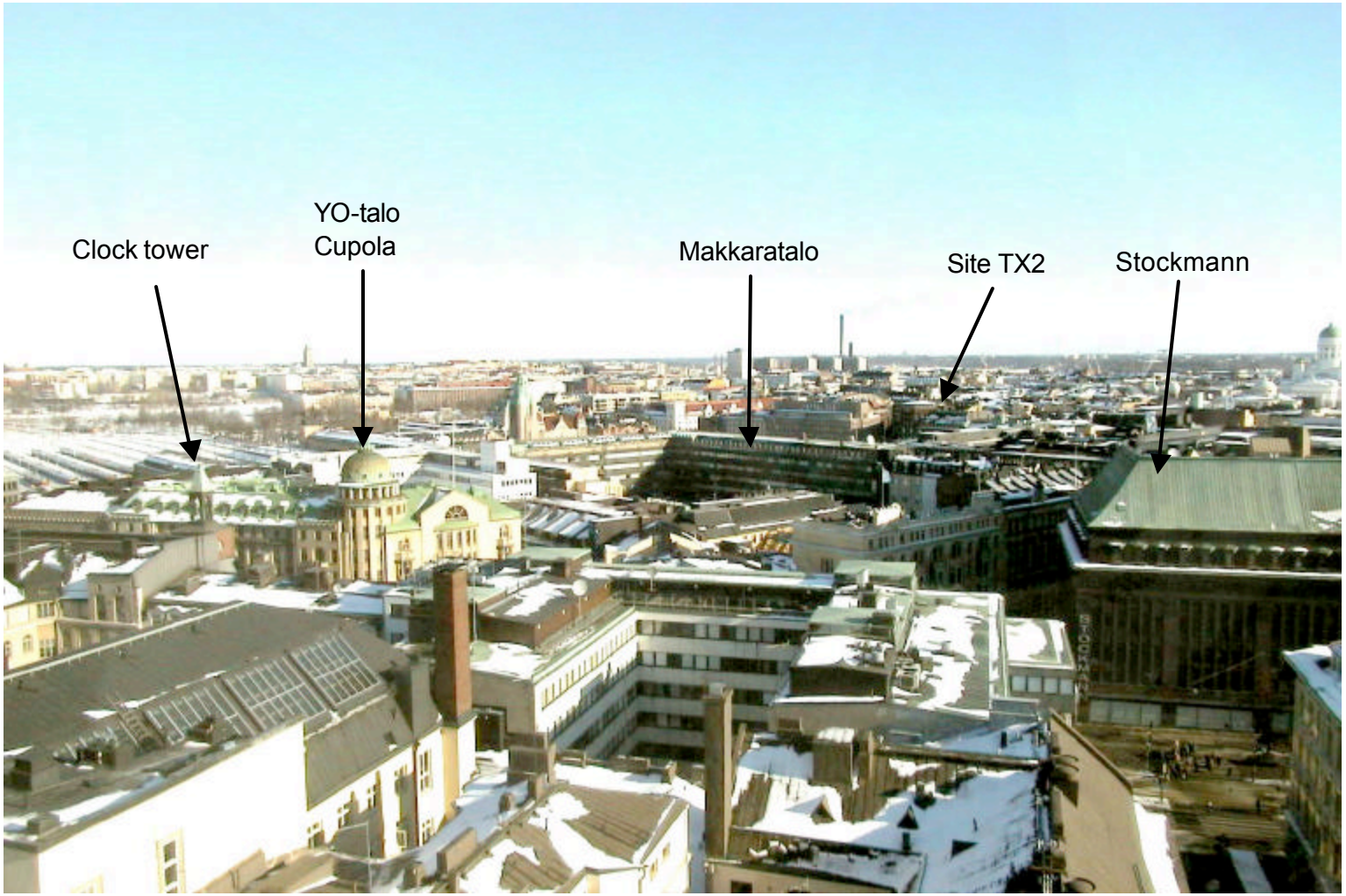

Figure 10. Measurement area of site TX2 seen from Hotel Torni.

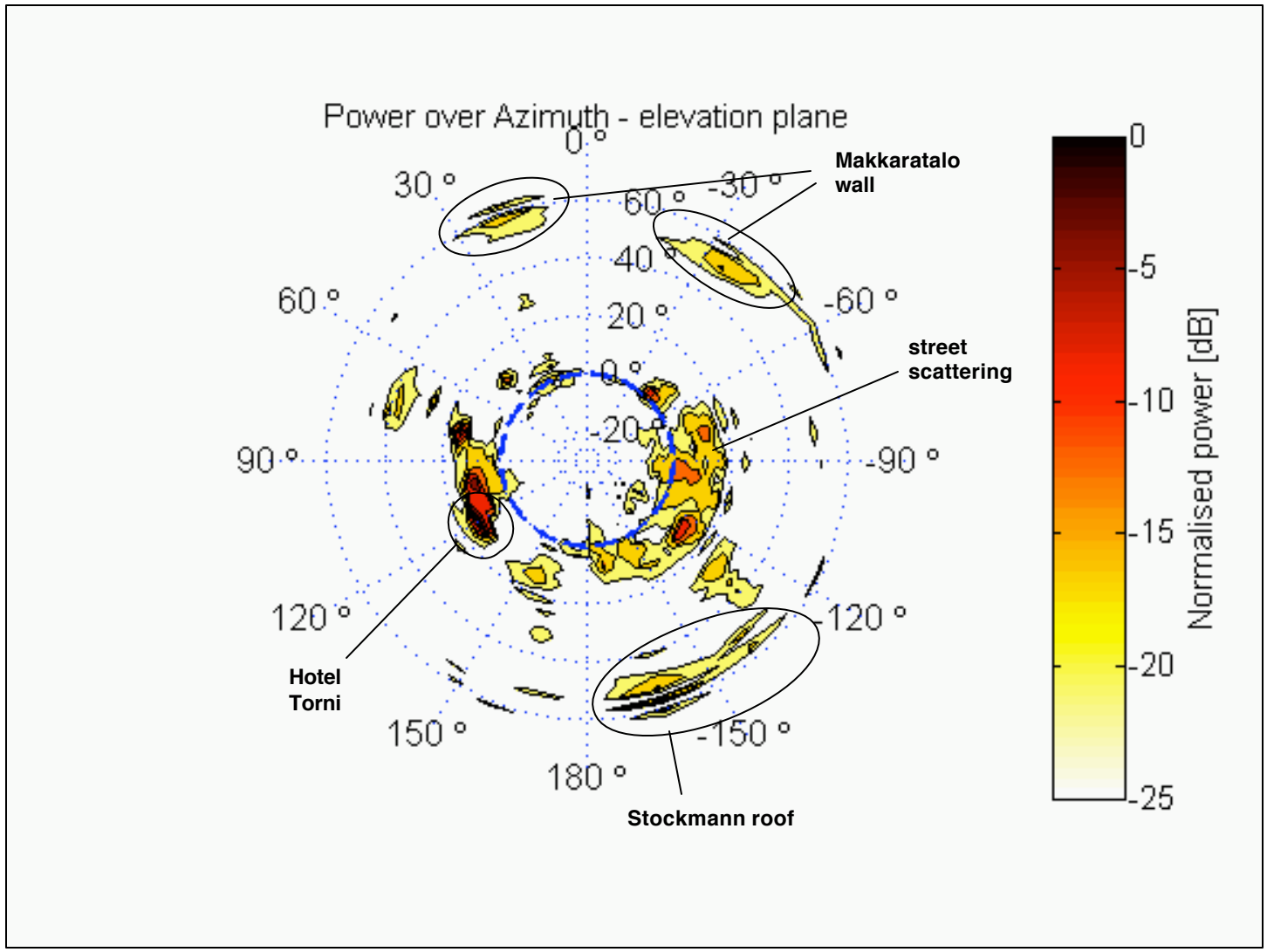

Figure 11. RX28 (TX2): Azimuth-elevation plane at mobile station.

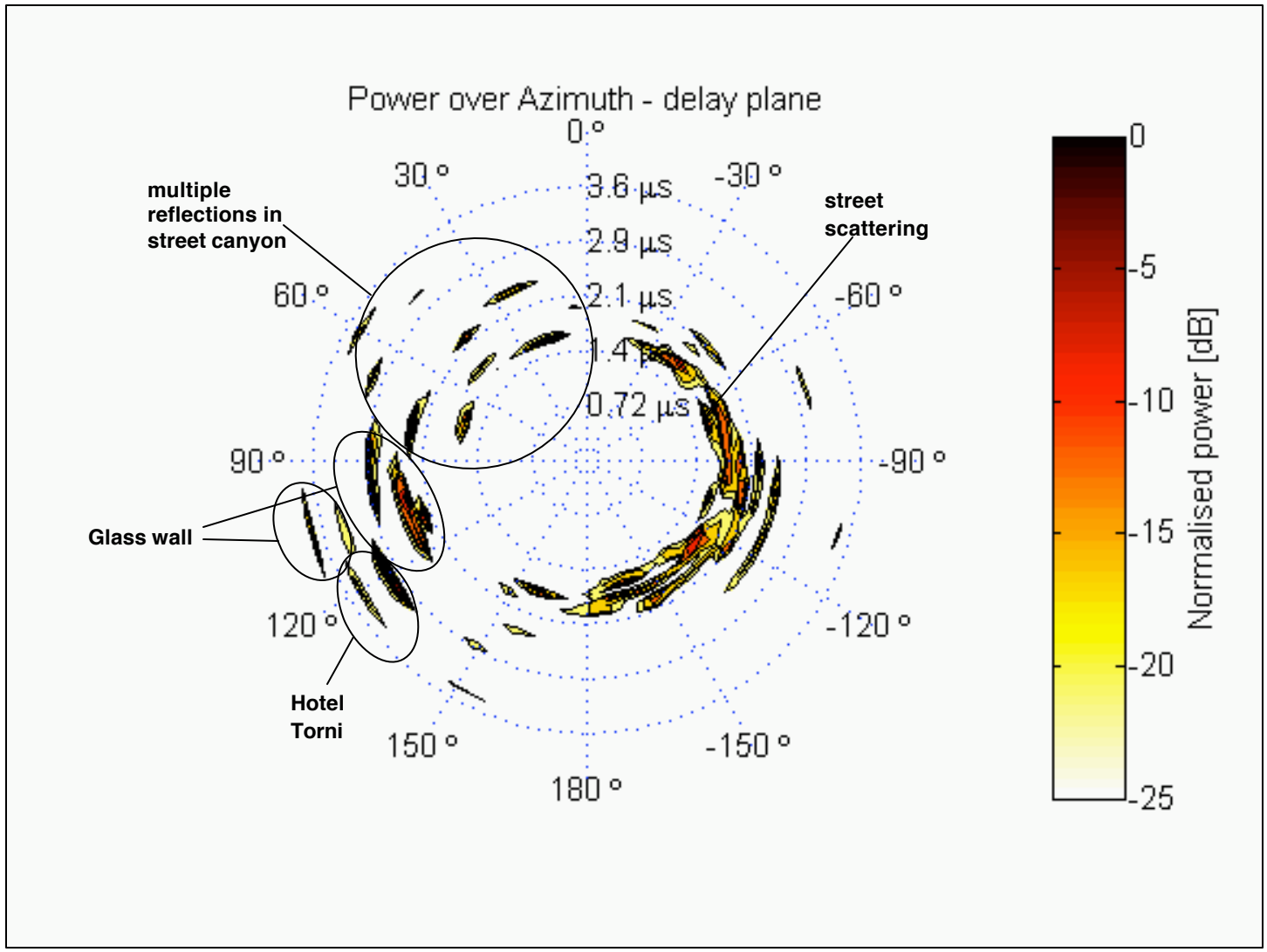

Figure 12. RX28 (TX2): Azimuth-delay plane at mobile station.

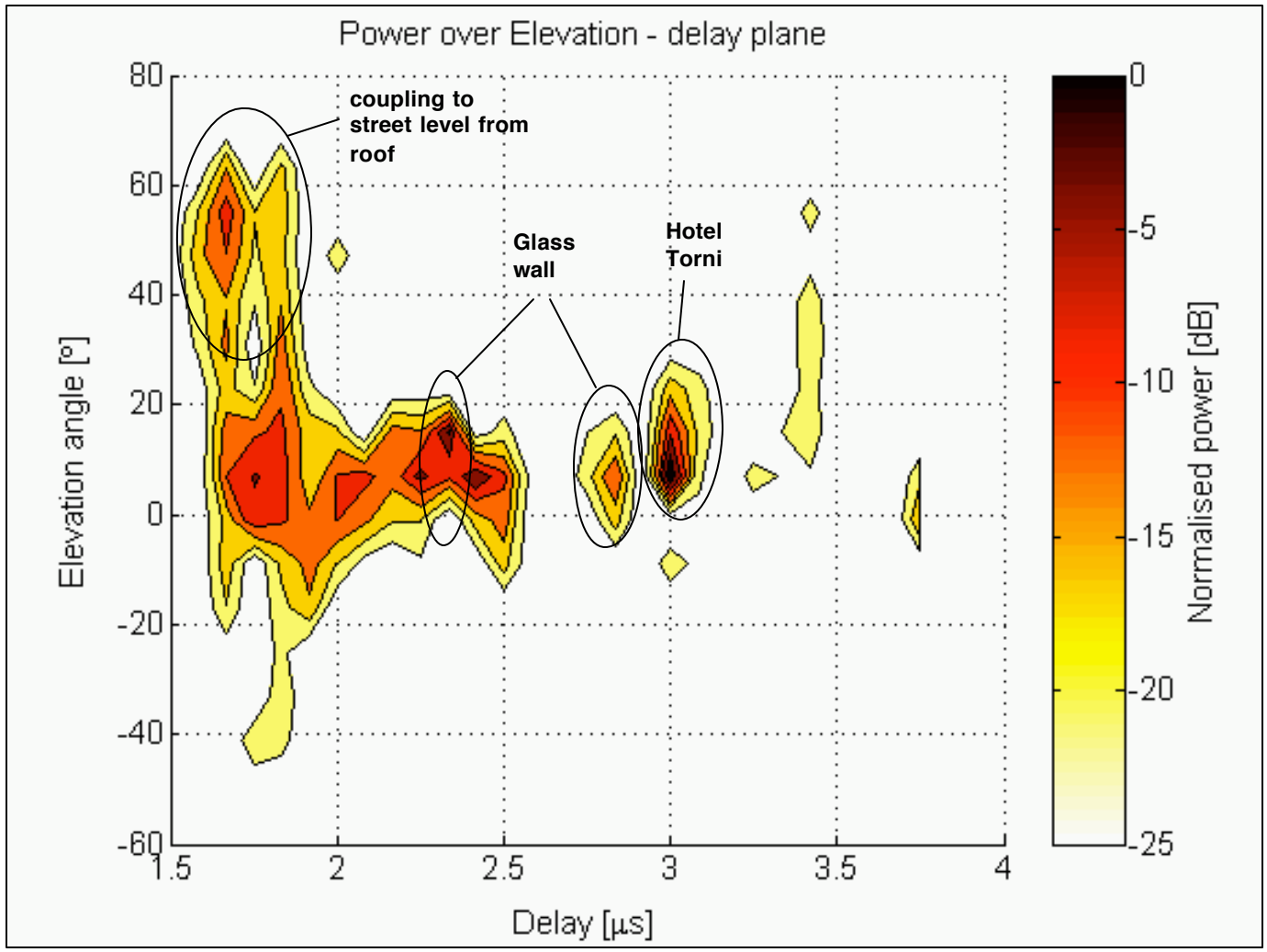

Figure 13. RX28 (TX2): Elevation-delay plane at mobile station.

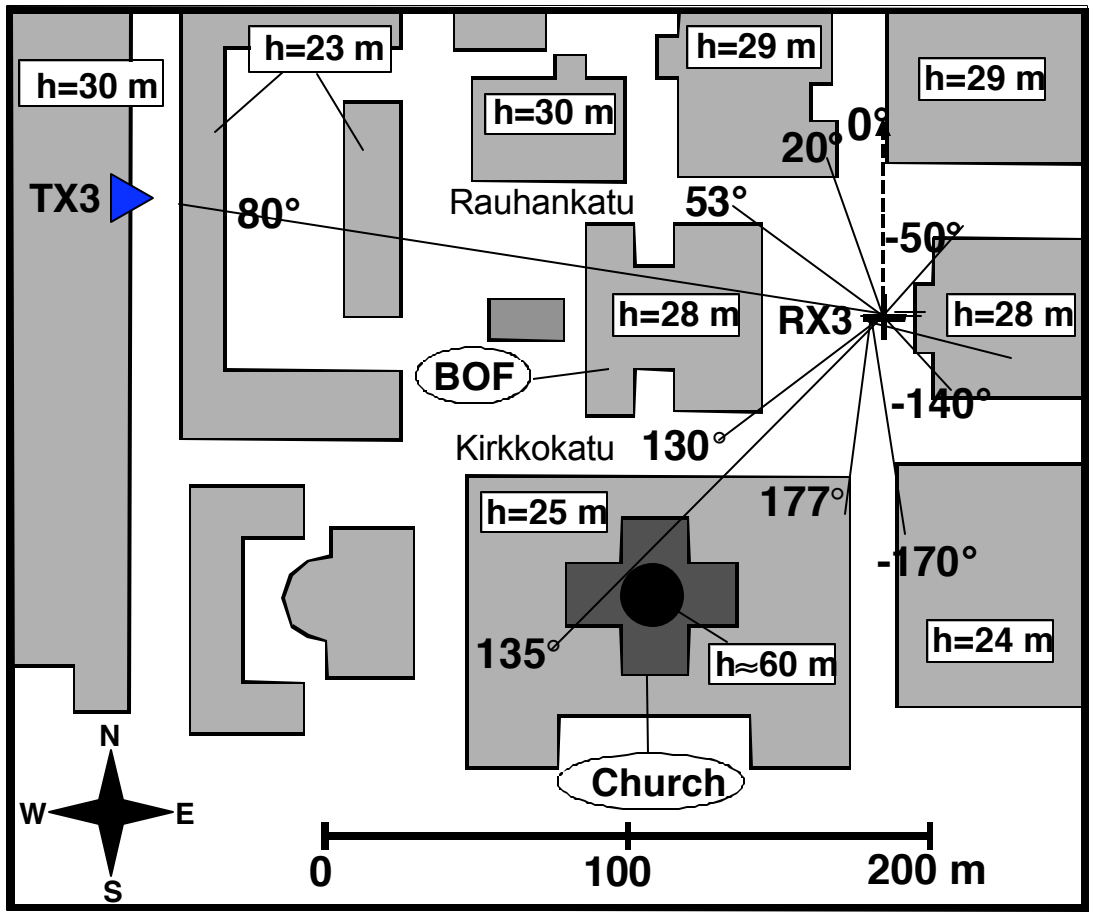

Figure 14. RX3 (TX3): Detailed map.

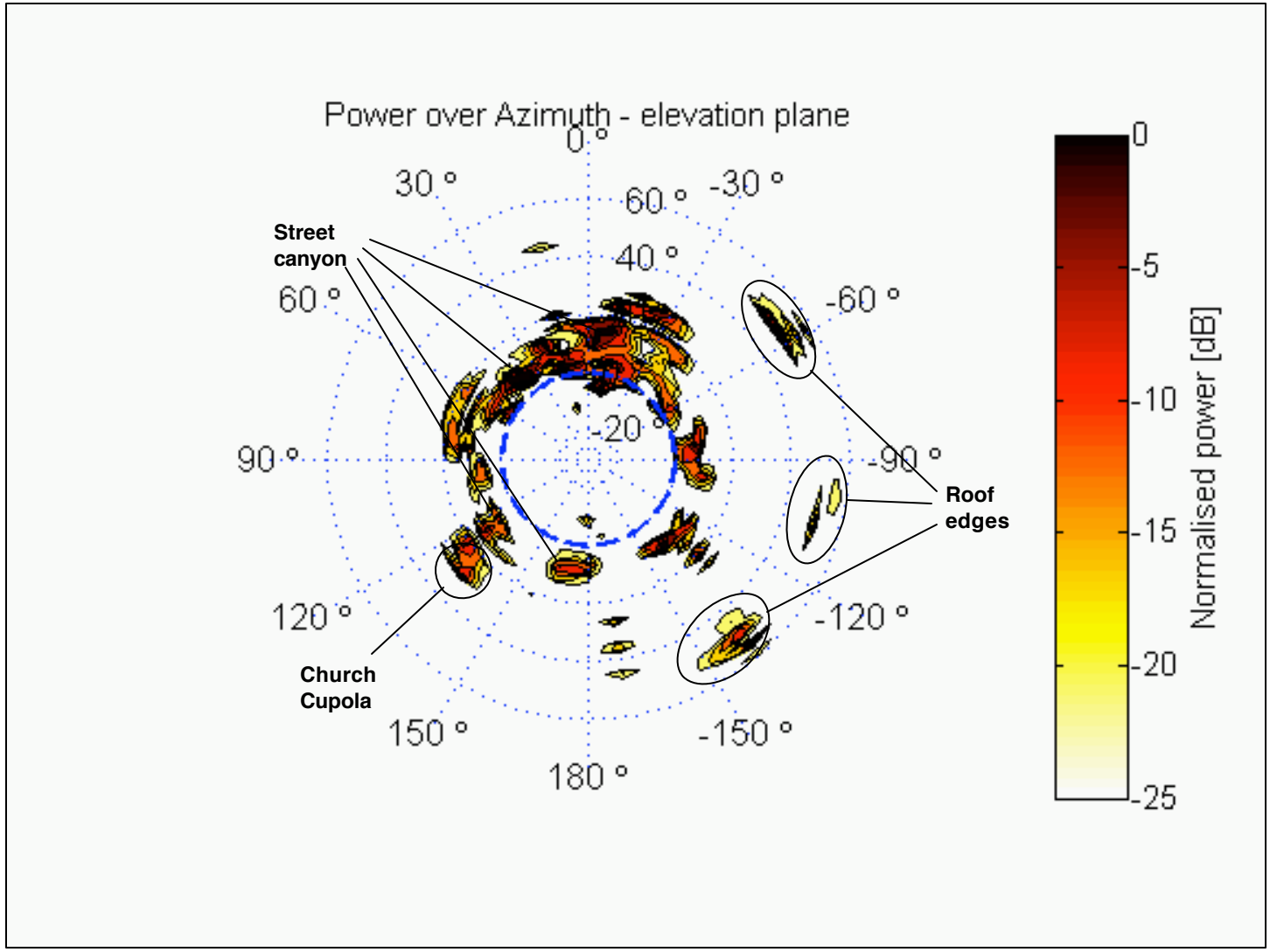

Figure 15. RX3 (TX3): Azimuth-elevation plane at mobile station.

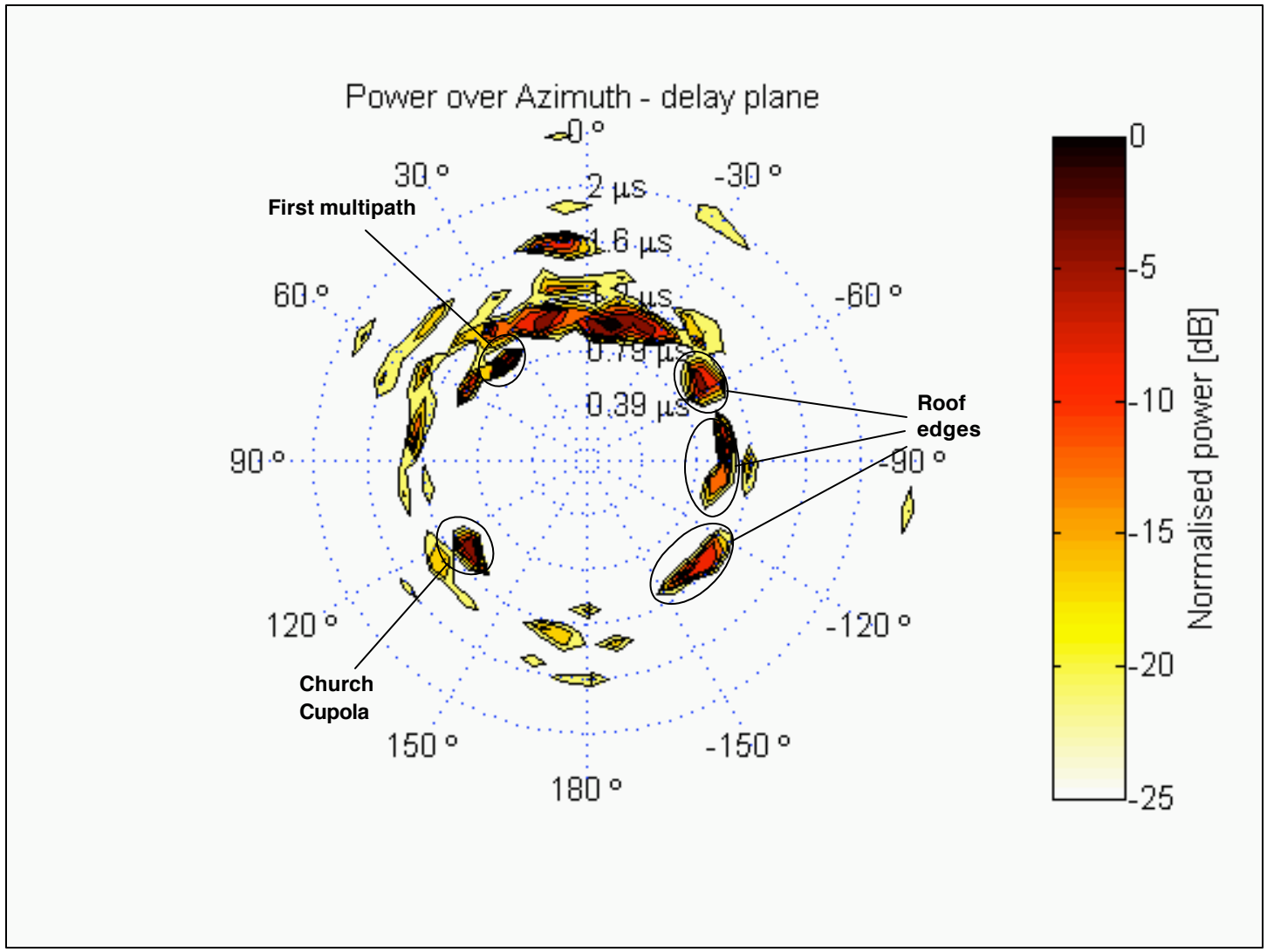

Figure 16. RX3 (TX3): Azimuth-delay plane at mobile station.

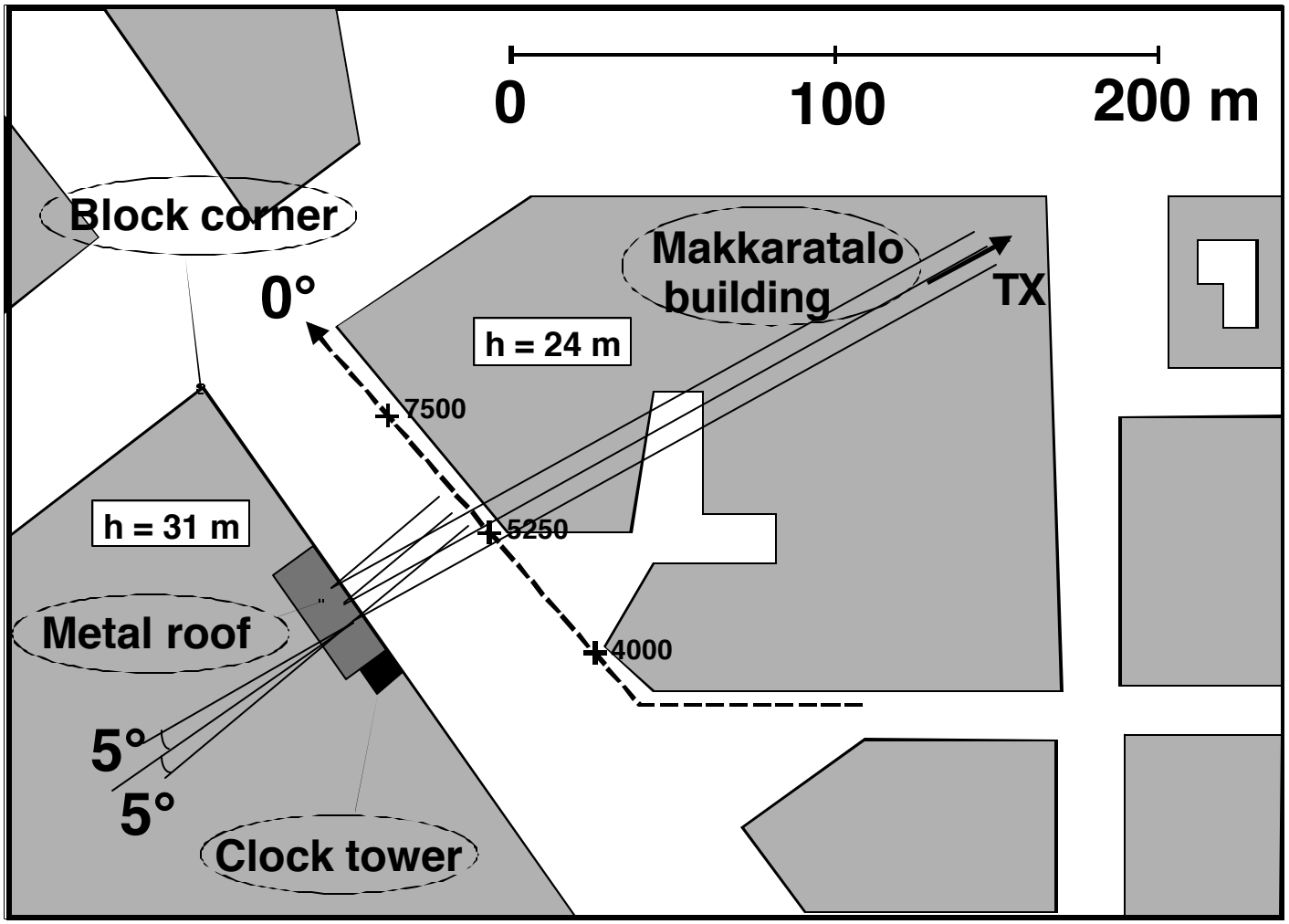

Figure 17. Continuous measurement route in street canyon.

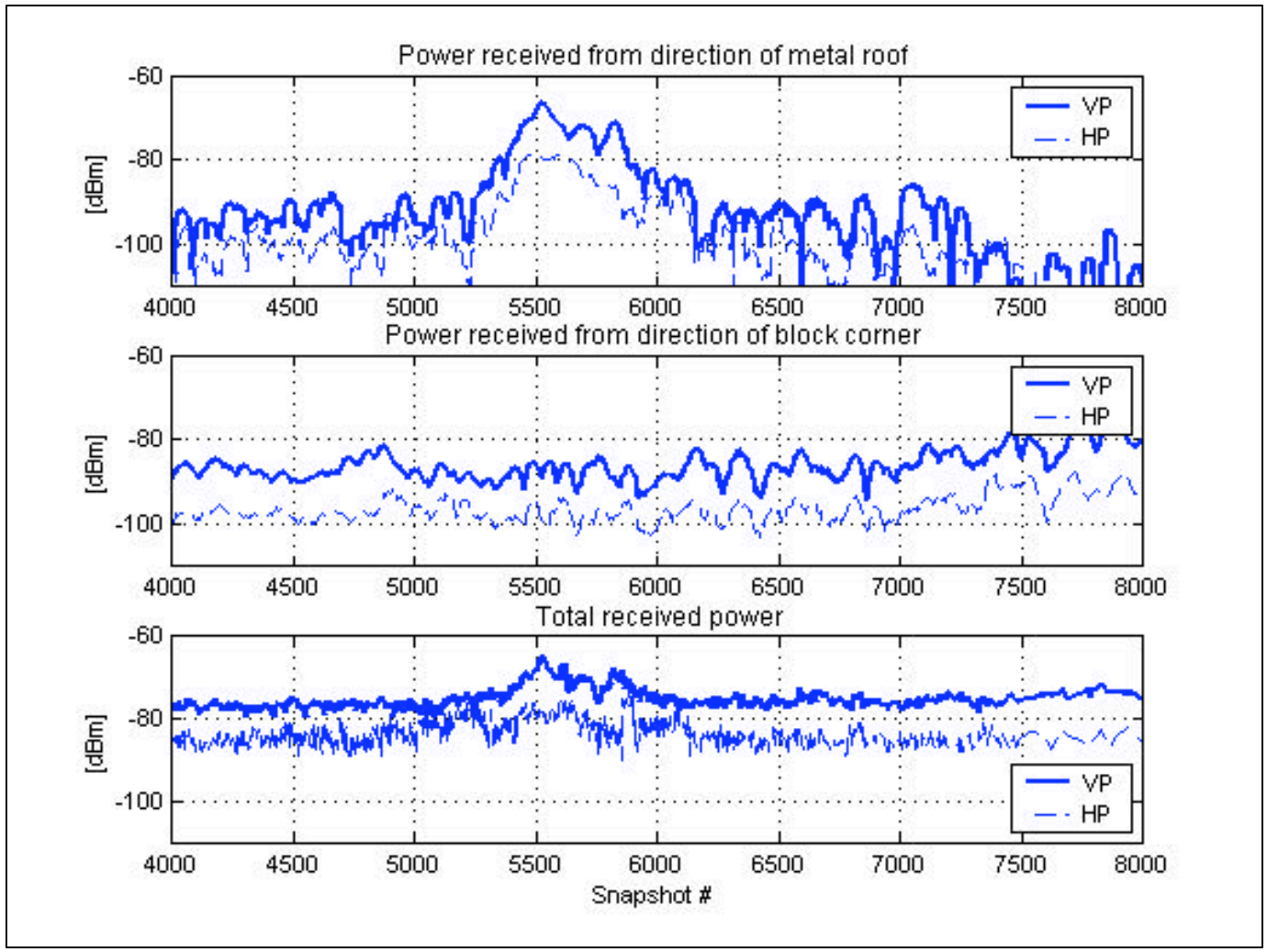

Figure 18. Power of different propagation paths along the route shown in Fig. 17.

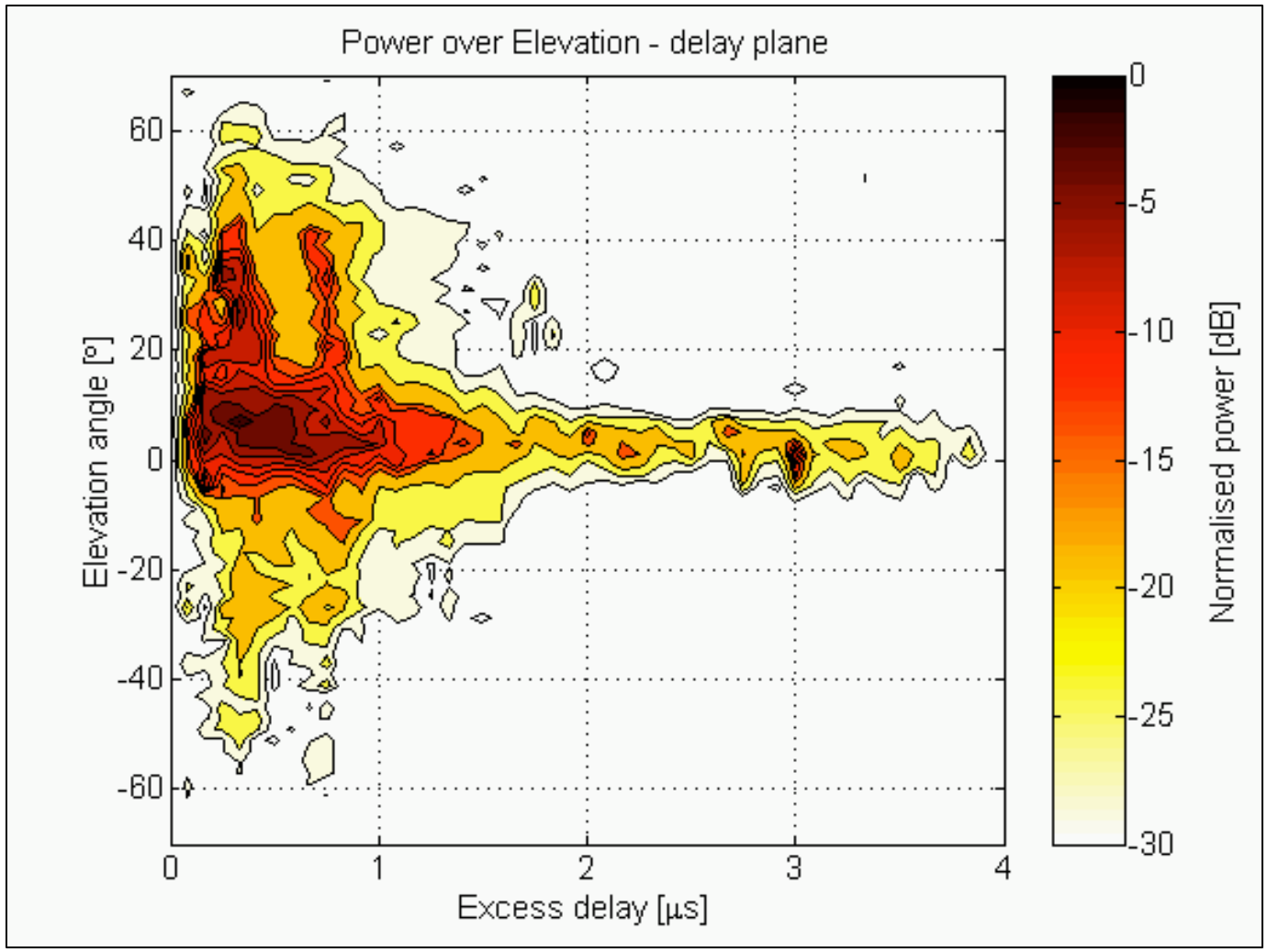

Figure 19. EDPP for excess delay averaged over all routes measured in street canyons.

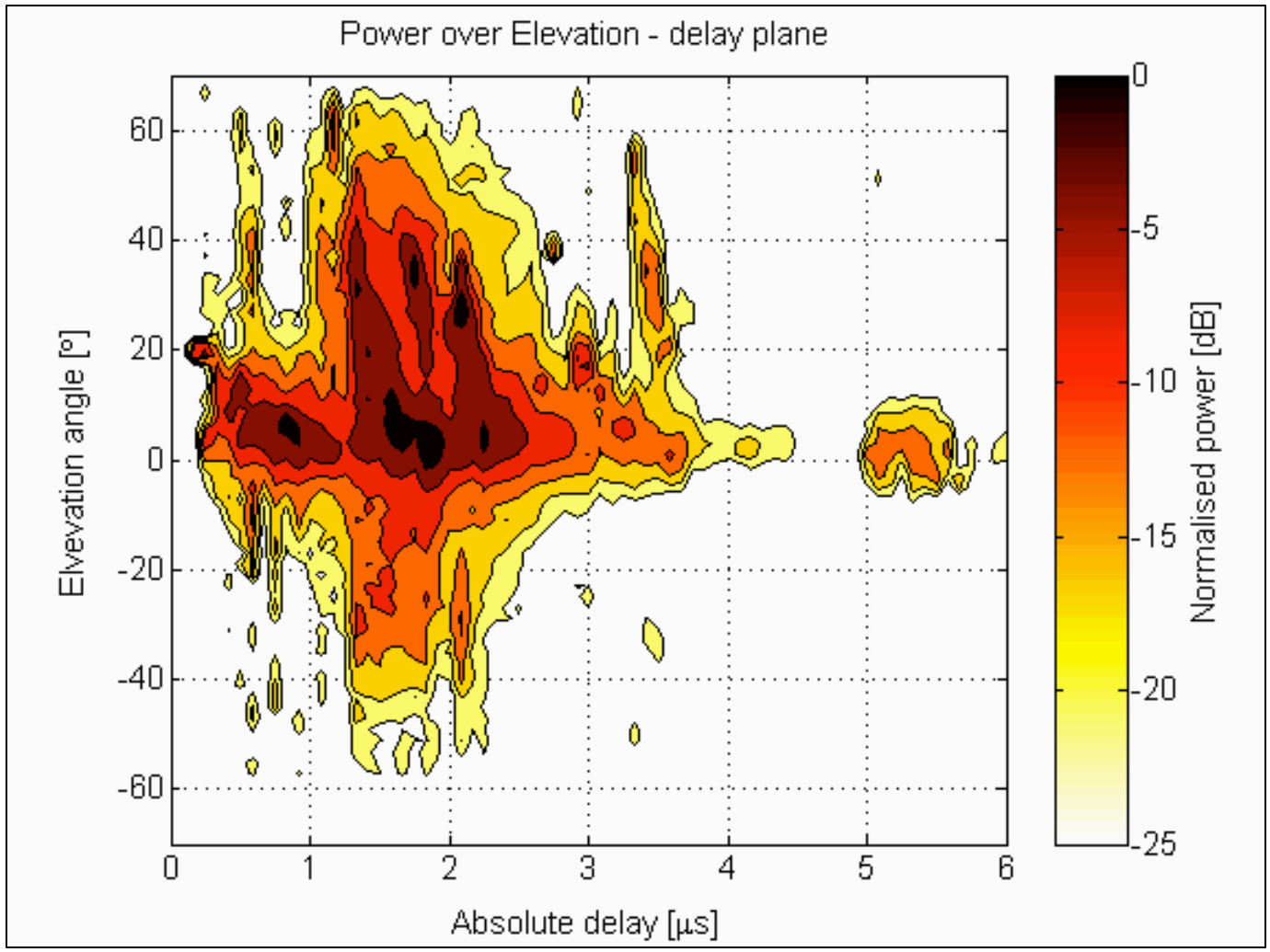

Figure 20. EDPP for absolute delay averaged over all routes measured in street canyons.

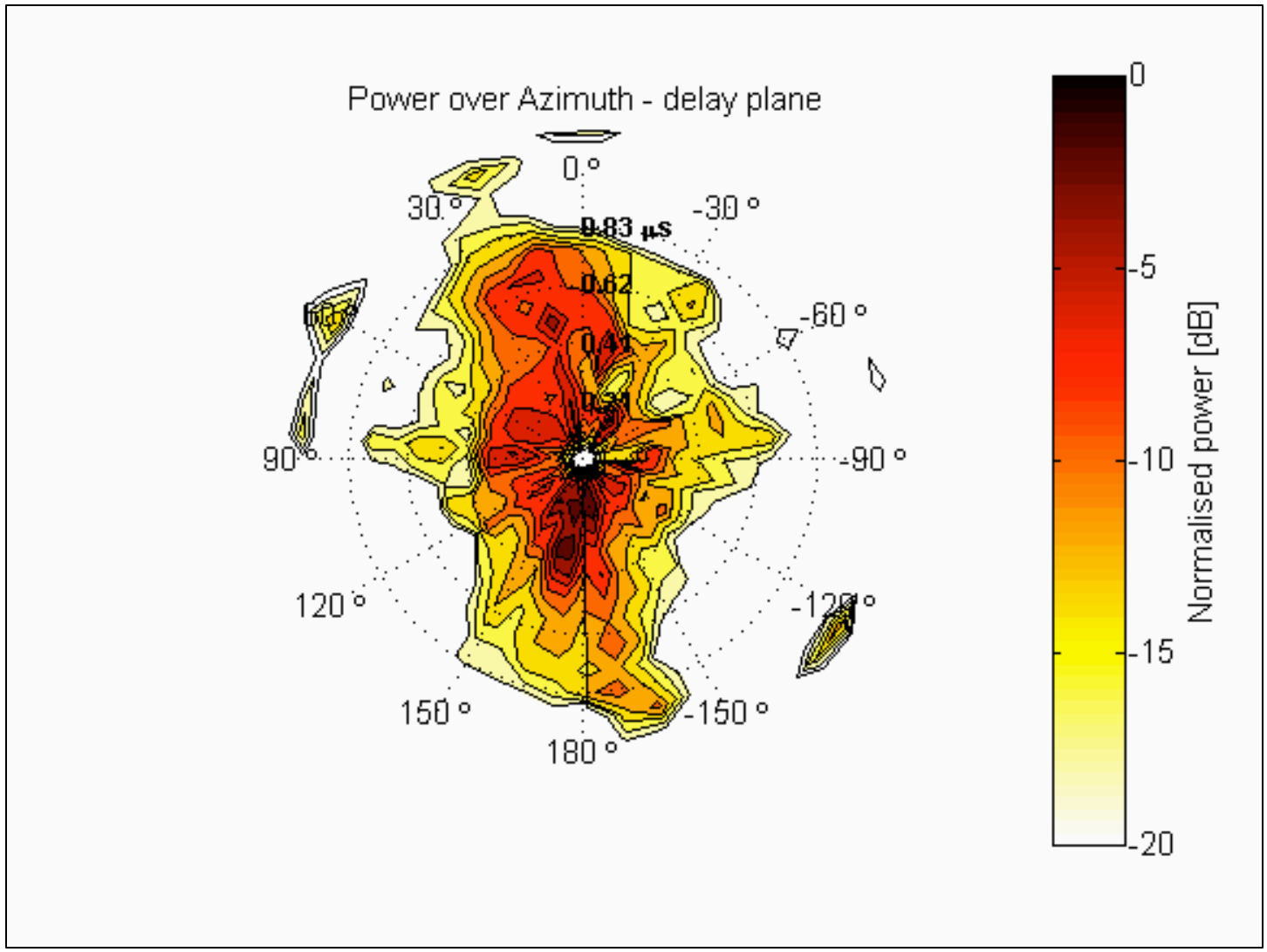

Figure 21. ADPP averaged over all data collected along routes in street canyons.